Contents list available at CBIORE journal website

International Journal of Renewable Energy Development

Journal homepage: https://ijred.cbiore.id

Research Article

Multi-criteria optimal sizing and analysis of PV/wind/fuel cell/battery/diesel generator for rural electrification: A case study in Chad

Mahamat Adoum Abdoulaye[a,b *], Sebastian Waita[a], Cyrus Wabuge Wekesa[c], Julius Mwakondo Mwabora[a]

[a]*Department of Physics, University of Nairobi, PO Box 30197-00100, Nairobi, Kenya*

[b]*Distributed Energy Team, Jeju Global Research Center, Korea Institute of Energy Research, (63357) 200, Haemajihaean-ro, Gujwa-eup, Jeju-si, Jeju, South Korea*

[c]*School of Engineering, University of Eldoret, PO Box 1125-30100, Eldoret, Kenya*

Abstract. Access to sustainable, clean, affordable, and reliable electricity is crucial for social and economic development, yet Sub-Saharan Africa (SSA) struggles significantly in this context. In CHAD, only 11.3% of the population is able to access electricity, making it one of the least electrified countries in SSA with the lowest clean energy access. In rural areas, electricity access falls to just 1.3%. This research applies and executes a Multi-Objective Particle Swarm Optimization (MOPSO) algorithm using MATLAB R2023b to assess the techno-economic, environmental, and social impacts of a hybrid system based on optimal PV/Wind/Battery/Fuel Cell (FC)/Diesel generator (DG) sizing for rural electrification in CHAD. The proposed system's self-sufficiency index (SSSI) and the Annualized System Cost (ASC) were chosen as objective functions to guarantee the economic feasibility of the system, higher self-sufficiency, and lower dependence on external energy sources (DG). The simulation results show that the optimal size of the proposed system supplies the load demand by 100% of the renewable energy sources (RES) fraction, and the optimal capacities of the main components to supply the load demand are: Solar Power (493 KW), Wind Turbine (166 KW), Battery Energy Charge/Discharge (229180 kWh /221300 kWh), Hydrogen tank storage energy (83 874 kWh), Electrolyzer size (202 KW), Fuel cell size (144 KW). The evelized cost of electricity (LCOE) of 0.2982 $/kWh, which is 51.12% lower than the national unit production costs of electricity in rural areas of CHAD (0.61 $/kWh). This LCOE is also the lowest compared to previous works done using HOMER Pro for the country of CHAD. The results also give a levelized cost of hydrogen (LCOH) of 3.8563 US $/kg, lower than for all studies found in the literature for the country of Chad. The proposed system's yearly avoided greenhouse gas (GHG) emission is 374 640 kg. The proposed system will create five (5) new jobs (JCO) and improve the Human Development Index (HDI) of the study area by 17.66% (the obtained HDI is 0.4683, and the CHAD HDI is 0.398) with an SSSI of 51.14%. This study provides a better practical energy design tool in decision-making for designers, companies, investors, policymakers, and the Chadian government when implementing this type of system in particular rural locations.

Keywords: Avoided greenhouse gas (GHG), social assessment, Hybrid energy system, Optimal sizing, rural electrification, Particle Swarm Optimization algorithm, zero-carbon electricity.

Received: 27th February 2024; Revised: 6th April 2024; Accepted: 15th April 2024; Available online: 18th April 2024

1. Introduction

Access to contemporary energy is critical for economic and social development, but Africa confronts significant difficulties in this regard. Due to the usage of environmentally harmful energy sources like wood and charcoal coupled with restricted access to clean energy resources, SSA is for instance, characterized by economic retardation and poverty (Agoundedemba et al., 2023). CHAD ranks among the countries with the lowest levels of electrification in SSA, with only 11.3% of its population has electricity access. This proportion of the population with electricity access is considerably lower in remote areas of CHAD (1.3%) (The World Bank Group, 2021). Based on a comparison of the 35 SSA nations' social index of access to clean energy (Social CEA), Chad is ranked last on the list (Casati *et al.*, 2023). This lack of access clean energy negatively influences education, communication, and access to quality care. Traditional energy sources can only satisfy the demand for electricity by addressing the difficulties harmful emissions of gases as well as elevated fuel life cycle costs (Bahramara *et al.*, 2016). Renewable energy sources (RES) are accessible, inexhaustible, and eco-friendly. As the world's population continues to grow and the imperative to decrease carbon dioxide (CO_2) emissions intensifies, the search for sustainable and renewable energy is expanding rapidly globally (Shafiullah *et al.*, 2021); (Hassane *et al.*, 2022).

Accelerating rural electrification is an efficient strategy for lowering carbon dioxide emissions. One of the most prominent RES under consideration is photovoltaic (PV) electricity generation (Fu, 2022). Zhang et al. concluded from their

* Corresponding author
Email: mahamatadoumabdoulaye1@gmail.com (M. A. Abdoulaye)

https://doi.org/10.61435/ijred.2024.60169
ISSN: 2252-4940/© 2024.The Author(s). Published by CBIORE

experiment that wind energy integration can affect the reduction of CO_2 emissions via the use of hydrogen-energy storage (Y. Zhang & Yu, 2022). Due to the variability of RES, combining an energy storage system (ESS) with RES is an option for increasing system reliability (Wang *et al.*, 2021). Currently, electrochemical energy storage systems (ESS), such as lithium and lead-acid batteries, dominate the market (Xu et al., 2022). For instance, these electrochemical ESS are unsuitable for the long-term storage necessary for RES because they are only cost-effective for short-term storage. Also, their technological progress may be limited because they need more lithium and cobalt, which are essential parts of their technology (Albertus *et al.*, 2020); (Olivetti *et al.*, 2017). As a result, there has been a search for various ESS alternatives that can work in hybrid or independently (Bocklisch, 2015). The green hydrogen storage system is one of the most often used alternatives nowadays due to its environmentally friendly nature and minimal environmental footprint, and hydrogen may be transported to the desired area if storage is low (Al-Buraiki & Al-Sharafi, 2022; J. Li *et al.*, 2022). According to (Delano *et al.,* 2020; (Aziz *et al.*, 2019); León Gómez *et al.*, 2023), a hybrid off-grid system proves to be a more reliable and economical option for rural electrification compared to a single energy source system.

Many previous works in the subregion have been carried out in modeling and optimizing hybrid RES, considering hydrogen and/or battery storage options with various configurations and methods. To the best of our knowledge, only few have been carried out for some sites in Chad (Diop et al., 2019); Wu *et al.,* 2019; Jahangiri *et al.,* 2019; Hassane *et al.*, 2022; Hassane, Didane *et al.,* 2022; Kelly *et al.*, 2023).

In (Hassane *et al.*, 2022; Hassane, Didane *et al.,* 2022), the authors compared and analyzed six different hybrid system scenarios across five remote locations in Chad to evaluate the technical, economic and environmental viability. In (Kelly et al., 2023), using HOMER software, the authors modeled and simulated a hybrid system comprising off-grid PV/DG/Wind/Batteries, which was evaluated across 16 unelectrified regions in Chad, taking into account three distinct community load profiles for each region. (Diop *et al.*, 2019) Designed and evaluated the technological, economic, and ecological dimensions of a hybrid system that includes PV panels, winds, diesel generators, and batteries for three climatic regions of Chad using HOMER. In (Wu *et al.*, 2019), The authors explored the viability of using solar/wind/DG/batteries to meet the energy requirements of Amjarass (a Chadian town), And in (Jahangiri *et al.*, 2019), the authors evaluated the Grid-connected PV/Wind/Hydrogen storage system feasibility to supply electricity in 25 locations across Chad.

However, there are some limitations to these previous works: in (Jahangiri *et al.*, 2019), even though 25 Chadian locations were taken into account, only a single load profile was utilized for each location. Although the four potential load profiles in each of the three climatic zones of Chad were examined by (Diop *et al.*, 2019), the authors assumed that the Faya, Pala, and Abeche sites were indicative of the entire country. (Wu *et al.*, 2019) focused their study on a single site, Amjarass, and examined one hypothetical load profile.

None of the works done in Chad has explored off-grid PV/Wind/Battery/FC/DG systems for rural electrification. Also, all these previous works focused on techno-economic and environmental factors, and none of them considered social criteria, especially the job creation opportunities and the improvement of the Human Development Index by their proposed systems.

To fill these gaps identified in the prior studies, we propose a multi-criteria hybrid system to electrify rural areas within the scope of Chad by considering fourteen (14) sub-criteria. For the technical criteria, five (5) sub-criteria have been considered: The System Self-Consumption Index (SSCI), the System Self-Sufficiency Index (SSSI), the Loss of Load Probability (LOLP), the unmet load, and the energy excess. For the economic criteria, we considered the Net Present cost (NPC), the Levelized Cost of Energy (LCOE), the Levelized Cost of Hydrogen (LCOH), and the fuel cost. The environmental criteria evaluate the avoided carbon dioxide (CO_2) and the renewable energy fraction. The new job creation opportunity, the Human Development Index (HDI) improvement, and the social acceptance have been considered as social criteria.

The objective of this research is to perform a techno-economic, environmental, and social analysis of a multi-criteria hybrid system based on optimal sizing of solar photovoltaic (PV), wind, battery, fuel cell, and diesel generator (DG) for rural electrification in CHAD using a multi-objective particle swarm optimization (MOPSO) algorithm that is implemented and runs in the MATLAB R2023b environment.

2. Materials and method

2.1 Problem statement and significance of the study

Chad ranks among the countries with the lowest electrification rates globally, with just 11.3% of its populace having electricity access. In Chad's rural regions, this figure drops significantly to merely 1.3% (The World Bank Group, 2021). Furthermore, in Chad, 75% of the population continues to reside in remote regions (Hassane *et al.*, 2018; Hassane *et al.*, 2022), so access to electricity enables the population to have lighting after sunset, significantly extending the duration of productive tasks. It also provides households with the opportunity to adopt clean cooking techniques, as opposed to the hazardous and polluting fuels like wood and charcoal, which are commonly used by the large portion of the rural population in Chad (Hassane *et al.*, 2019). The absence of electricity in rural areas of Chad adversely affects education, communication, access to quality care, and the Human Development Index (HDI). Chad's HDI stands at 0.398, categorizing it under "low human development" globally, ranking 187th among 189 countries and territories (PNUD, 2020). Rural electrification in Chad encounters several challenges (technical, economic, environmental, and social) that need to be overcome. A major hurdle is financing, given the country's insufficient resources to support costly electrification initiatives. Additionally, the inadequacy of electricity infrastructure in rural regions presents further difficulties, especially since the population is spread out across Chad's countryside (Djounga, 2023). Sustainability is a crucial concern, as climate change may impact the stability and longevity of the electricity grid. The absence of sustainable and decentralized electrification systems in Chad's rural areas is a significant and urgent problem (Mbainaissem *et al.*; PNUD, 2014). The cost of electricity is a major issue, as the electricity supplied by Chad's National Electricity Company (SNE) is among the highest-priced in Central Africa. The average resale price per kilowatt-hour (kWh) stands at 157 F CFA (0.25 USD), yet it is sold at a loss due to the SNE's unit production costs ranging from 252 F CFA to 375 F CFA (0.41 to 0.61 USD) per kWh in urban and rural areas, respectively. This pricing structure hinders the population's access to electricity (Abdelhamid, 2023). The National Electricity Company (SNE) of Chad is limited to producing and distributing electricity in just 7 out of the 23 regions in Chad, leaving 16 regions without electricity. Many remote areas in Chad still struggle with accessing electricity. The constant availability of power is a challenge because of the elevated costs of fuel and insufficient electricity infrastructure. In certain rural parts of Chad, electricity is available to the population for approximately four

Table 1
Load profile for the studied area by types of households by category of consumption

Type 1 households					
Devices used by the households	Lamps	Phone charge	Television	Ventilator	Fridge
Power (W)	40	20	200	40	200
Number of devices	3	1	0	0	0
Duration of use (hour/day)	6	2	0	0	0
Total power (W)	120	20	0	0	0
Daily Energy (Wh) by device	720	40	0	0	0
Type 2 households					
Devices used by the households	Lamps	Phone charge	Television	Ventilator	Fridge
Power (W)	40	20	200	40	200
Number of devices	5	1	1	0	0
Duration of use (hour/day)	6	2	4	0	0
Total power (W)	200	20	200	0	0
Daily Energy (Wh) by device	1200	40	800	0	0
Type 3 households					
Devices used by the households	Lamps	Phone charge	Television	Ventilator	Fridge
Power (W)	40	20	200	40	200
Number of devices	3	1	1	2	1
Duration of use (hour/day)	6	2	4	8	8
Total power (W)	120	20	200	80	200
Daily Energy (Wh) by device	720	40	800	640	1600

Source : (Hassane *et al.*, 2022)

hours daily, between 6 p.m. and 10 p.m (Kelly *et al.*, 2023). The lack of affordable and reliable electricity severely restricts development, perpetuating poverty, slowing education, and limiting economic opportunities for the Chadian rural community.

Considering all the above Chadian rural electrification challenges, this study addresses a techno-economic, environmental, and social analysis based on PV/Wind/Battery/Fuel Cell/DG using a MOPSO algorithm. The proposed optimization model aims to balance the energy between the demand for power and its supply and the charging process of battery and hydrogen storage by defining the installed capacities of the main components, and Diesel generator while minimizing the ASC and maximizing the SSSI and obtaining the values of the other sub-criteria which serve as decision-making variables for this feasibility analysis. primary objective of this research is to maximize the use of PV, Wind, Battery, and hydrogen while minimizing the use of Diesel generator.

2.2 Study area, load profile, and meteorological data

The present study was carried out in KOUNDOUL, Chari Baguirmi, with geographical coordinates 11° 58′ 35″ North and 15° 09′ 00″ East, where live (5,000 - 9,000) people in the rural area of the sahelian zone of Chad.

In this study, to perform the optimization outcomes for the PV/Wind/Battery/Fuel cell/Diesel generator, the PSO algorithm needs extra input data, such as the hourly load profile (Figure 1) and the meteorological data of the study area collected from the Photovoltaic Geographical Information System (PVGIS) website (Figures 2), and the characteristics techno-economic of components collected from the literature (Table 2).

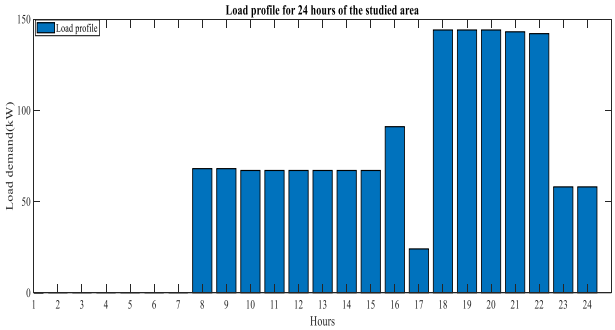

Fig. 1 Load profile for 24 hours of the studied area

Figure 1 shows the load profile for 24 hours of the studied area. From Figure 1, we notice that the peak load demand for the studied area is between 6 p.m. and 10 p.m. with a value of 144 KW. The average load is reached at 4 p.m. with a value of 91 KW. The minimum low load profile is reached at 5 p.m. with a value of 24 KW. The particularity of these three types of households is that the load consumption is zero from 1 a.m. to 7 a.m. 30.

Figures 2 represents the 24 hours meteorological data, respectively, the solar irradiance, wind speed, and the ambient temperature of the studied area. From this Figure 2, we can also note that the maximum and minimum solar irradiance, wind speed, and ambient temperature are 1017 W/m^2 and 0, 4.14 m/s and 2.62 m/s, 29.37 ^{0}C and 16.19 ^{0}C.

Table 1 shows the three types of household load profiles used in this study that represent low, medium, and high community consumers obtained through a survey (Hassane, Didane *et al.*, 2022). In the context of Chad, these three types of households can be identified in the country's rural and non-electrified areas.

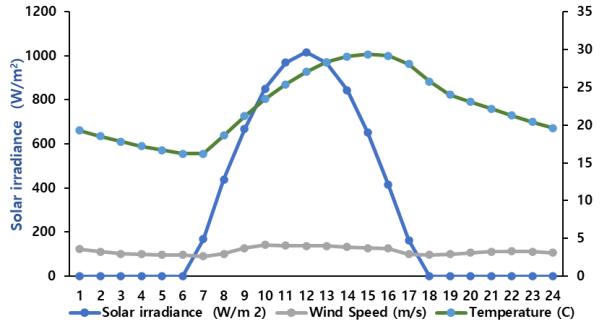

Fig. 2 Studied area's meteorological data for 24 hours

2.3 System configuration, Control strategy, and energy management system

2.3.1 Presentation of the proposed system configuration

The proposed system's schematic configuration considered in the present study is illustrated in Figure 3. In this system, the load requirement is met by RES, Battery (BES), Fuel Cell (FC), and Diesel Generator (DG) as a backup. Direct current (DC) bus is used as the connector of PV panels, Wind, FC, BES, Hydrogen Tank (HT), and Electrolyzer. Electrolyzer utilizes input power from PV panels/Wind to generate green hydrogen, this hydrogen is then converted into electrical energy through a fuel cell, which is used to meet energy demands. The proposed system have electrical demand, i.e., or alternative current AC. Therefore, converters are utilized for converting energy from DC to AC, and satisfy the power demand.

With this proposed system configuration, we obtained a completely autonomous electrical grid integrating zero-carbon electricity generation (PV and Wind). We are thus talking about an "island" mini-local grid (off grid) with low short-circuit power. This proposed system with a continuous common bus configuration is more suitable for small power island generation, which matches the need of the Chadian rural area power requirement.

The main advantages of the proposed system are the complementarity of resources, particularly wind and solar, whether on an annual or daily scale, more reliable energy availability, and environmental efficiency.

One of the goals of this research is to maximize the use of solar, wind, battery, and hydrogen, respectively, and minimize the use of diesel generators as much as possible.

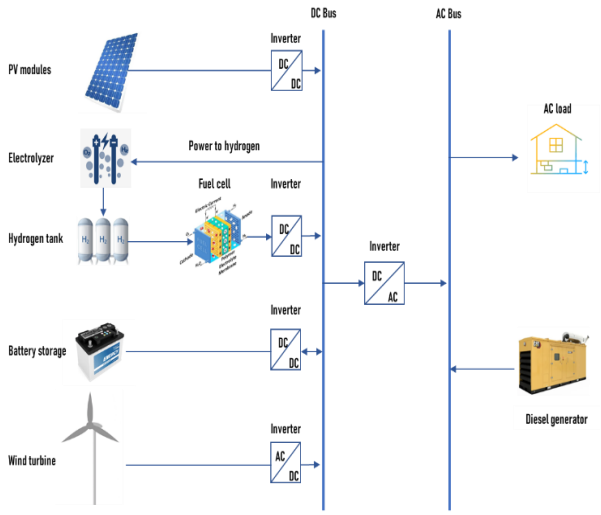

Fig. 3 Configuration of the proposed system: PV - Wind -Battery - Fuel cell – DG

2.3.2 Control strategy

The proposed model controls the energy flow management of different technologies (BES, PV, Wind, and FC), to fulfill the load requirement with maximum efficiency. In this standalone model, if the electricity from PV/Wind/FC/BES unable to supply the load, the missing load will be supplied by the DG. i.e., $(P_{PV}(t) + P_{WT}(t) + P_{FC}(t) + P_{BES}(t) < P_{load}(t))$.

A novel MOPSO algorithm is used as the control dispatch. The model determines the optimal dimensions for each component and the optimal control of the power distribution among the components.

The proposed control dispatch aims to balance the energy between power consumption and provision, and the charging process of battery and hydrogen storage while minimize NPC. The working principles of the novel control dispatch were based on the design objective. As previously mentioned, the proposed model is aimed at designing an off-grid system (PV/Wind/FC/BES/DG) that maximizes the utilization of fuel cell power output and minimizes the cost.

The working principles of the proposed operating strategies are as bellow:

Case 1. If the combined produced power from PV + Wind surpasses the required load, the demand is supplied by the output power from RES, and the extra electricity charges the BES; otherwise, the excess electricity will be utilized for hydrogen production to store in the HT. The FC is still not turned on.

Case 2. If the produced electricity by PV + Wind surpasses the required load, the required load is fulfilled by the RES output, and BES is fully charged and HT is also filled. Then surplus energy is dumped.

Case 3. If the required load surpasses the PV + Wind power output, BES is discharged to fulfill load demand. The algorithm favors the RES and BES to satisfy the energy demand.

Case 4. In case of RES and BES cannot fulfill the power requirement, FC runs. i.e., $(P_{PV}(t) + P_{WT}(t) + P_{BES}(t) < P_{load}(t))$, The FC generates the excess power necessary to fulfill the specified load demand; i.e., $(P_{FC}(t) = P_{load}(t) - P_{PV}(t) - P_{WT}(t) - P_{BES}(t))$.

Case 5. If the electricity from PV/Wind/FC/BES unable to match the energy demand, i.e., $(P_{PV}(t) + P_{WT}(t) + P_{FC}(t) + P_{BES}(t) < P_{load}(t))$, then the missing load energy is purchased from DG.

2.3.3 Energy and power management system

Figure 4 shows the proposed system's energy management system flowchart. As mentioned above, the proposed control dispatch aims to balance the energy between power consumption and provision and the charging process of battery and hydrogen storage while minimizing NPC. The proposed algorithm aims to optimally design the system (PV/Wind/FC/BES/DG) that maximizes fuel cell power output utilization and minimizes the cost. The abbreviations used in the flowcharts are listed below:

$P_{WT}(t)$: Wind turbine power
$P_{PV}(t)$ / $P_s(t)$: Power of solar
$P_L(t)$: Power demand at time t
η_{Inv} : Inverter efficiency
$P_{ch}(t)$: Available power for charging the battery
$E_{ch}(t)$: Charged energy into the battery
$P_{distch}(t)$: Power intended for discharge from the

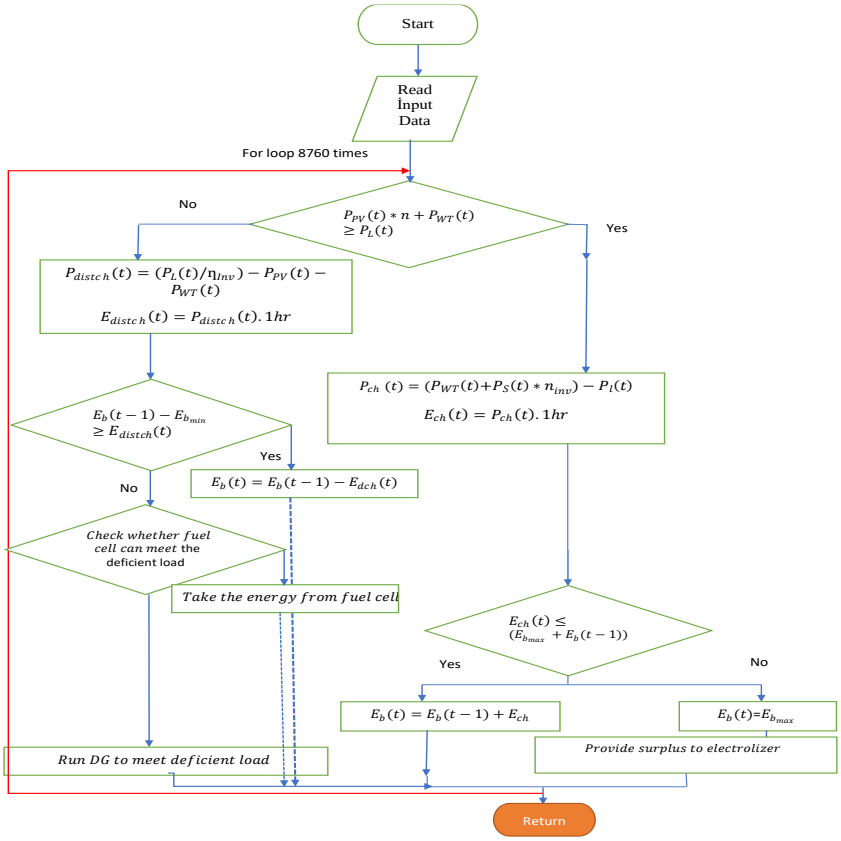

Fig. 4 Flowchart for the control strategy of the proposed system

battery
$E_{distch}(t)$: Battery discharged energy
$E_{b_{max}}$: Battery's maximum energy capacity
$E_b(t)$: Battery's energy level at time t
$E_{gridp\_s}(t)$: Supplied energy to the grid at time t
Input Data :Load demand, meteorological data, components characteristics, and techno-economic parameters.

2.4 Proposed system's mathematical modeling

2.4.1 PV generator modeling

The the equation (1) the PV generator output power (Talla Konchou et al., 2021; Islam et al., 2022; Wankouo Ngouleu et al., 2023) :

$$P_{PV}(t) = N_{PV} \times P_r \times \eta_{PV} \times \left(\frac{G}{G_{ref}}\right) \times \left[1 + \beta\left(T - T_{ref}\right)\right] \quad (1)$$

Here P_{PV} is the PV output power in (kW), Pr represents the estimated unit output in (kW), Npv is the quantity of PV panels, η_{PV} is the efficiency of the PV panel, G represents the entire irradiation in (kW/m²), Gref represents the standard solar irradiance in (1 kW/m²) under normal conditions (25°C), Tref is the temperature at the standard condition (25°C), β is the temperature coefficient of the PV cell at peak power, T is the PV cell's temperature (°C) as shown in equation (2) (Zhang et al., 2020; Koholé et al., 2023; Wankouo Ngouleu et al., 2023):

$$T = T_{am} + \left(\frac{NOCT - 20}{1000}\right) \times G \quad (2)$$

Where NOCT refers to the standard cell's operating temperature (°C) taken as 45°C under the following conditions in the study: Air mass (AM=1.5), Tam=20°C, and the solar radiation (G = 1000W/m²), Tam is the ambient temperature (°C) (Wankouo Ngouleu et al., 2023a).

2.4.2 Modeling of wind turbines

Equation (3) is utilized to determine the power output from the wind turbine (Alshammari & Asumadu, 2020; Kharrich et al., 2021):

$$P_{WT}(t) = \begin{cases} 0, & V(t) \leq V_{ci}, V(t) \geq V_{co} \\ P_r, & V_r \leq V(t) < V_{co} \\ a \times V(t)^3 - b \times P_r, & V_{ci} \leq V(t) < V_r \end{cases} \quad (3)$$

a and b represent two variables as outlined in equation (4):

$$\begin{cases} a = \dfrac{P_r}{\left({V_r}^3 - {V_{ci}}^3\right)} \\ b = \dfrac{{V_{ci}}^3}{\left({V_r}^3 - {V_{ci}}^3\right)} \end{cases} \quad (4)$$

Where PWT(t): wind turbine's generated power (kW), P_r is the calculated wind power (kW), Vci in (m/s) indicates the wind speed cutoff, Vco represents wind speed at which the wind turbine achieves its speed termination, measured in meters per second, Vr represents the estimated wind speed in meter per second, V(t) in (m/s) represents speed of wind at hub height and can be computed by utilizing equation (5) (Alshammari & Asumadu, 2020):

$$V(t) = V_r \left(\frac{H_{WT}}{H_r}\right)^{\alpha} \quad (5)$$

Where α: represents the parameter of friction, assuming a value of (1/7) for exposed locations and surfaces with little roughness, HWT: represents wind turbine's hub height, Hr: altitude.

The wind turbine's rated power (Pr) can be determined using equation (6) using wind turbine's swept area A, the maximum power coefficient (Cp), which ranges between 0.25 and 0.45% and the air density (ρ) (Kharrich et al., 2019; Guangqian et al., 2018):

$$P_r = \frac{1}{2} \times \rho(t) \times A_{Wind} \times Cp \times {V_r}^3(t) \quad (6)$$

2.4.3 Inverter modeling

According to (Mumtaz et al., 2021) the inverter power can be expressed in equation (7) :

$$P_{inv}(t) = \frac{P_L(t)}{\eta_{inv}} \quad (7)$$

Where $P_L(t)$ is the hourly load demand and η_{inv} is the efficiency of the inverter. The size of inverter is given by the equation (8) (Singh et al., 2020; Emad et al., 2021):

$$P_{inv,rated} = \frac{P_{L,peak}}{\eta_{inv}} \quad (8)$$

Where $P_{inv,rated}$ is the rated inverter 's power and $P_{L,peak}$ is the peak load.

2.4.4 Battery energy storage (BES) system modeling

The proposed system has a total hourly power output of equation (9):

$$P_T(t) = P_{PV}(t) + P_{WT}(t) \quad (9)$$

Where $P_{PV}(t)$ and $P_{WT}(t)$ are the hourly outputs of PV and wind turbines, respectively.

The battery battery charges when $P_T(t) > P_{load}(t)$, the battery SOC is given by equation (10) (Anoune et al., 2018; Diaf et al., 2007):

$$SOC_B(t) = SOC_B(t-1)(1-\sigma) + \big(P_T(t) - P_{inv}(t)\big)\eta_{BC} \quad (10)$$

Where σ is the battery's manufacturer-provided self-discharge rate, and η_{BC} is the battery charging efficiency.

However, When $P_T(t) < P_{load}(t)$, at that hour the battery is discharging, the battery SOC is given by equation (11) (Anoune *et al.*, 2018; Diaf *et al.*, 2007):

$$SOC_B(t) = SOC_B(t-1)(1-\sigma) - \big(P_{inv}(t) - P_T(t)\big)\eta_{BC} \quad (11)$$

Where η_{BD} represents battery's discharging efficiency and the charge/discharge process is always between the battery's maximum and minimum limitations, equation (12):

$$SOC_{Bmin} \leq SOC_B(t) \leq SOC_{Bmax} \quad (12)$$

The SOC_{Bmin} is given by equation (13):

$$SOC_{Bmin} = DOD \times SOC_{nominal} \quad (13)$$

Where $SOC_{nominal}$ is the nominal capacity, DOD represents the depth of battery's discharge. The maximum permitted state of a battery SOC_{Bmax} is equal to its nominal capacity $SOC_{nominal}$ according to equation (14):

$$SOC_{Bmax} = SOC_{nominal} \quad (14)$$

2.4.5 Electrolyzer modeling

The electrolyzer is used to convert electrical energy into hydrogen via electrodialysis processes. Hydrogen is produced by applying an electric current to water as shown in equation (15) (C. H. Li et al., 2009):

$$H_2O + electrcity \rightarrow H_2 + \frac{1}{2}O_2 \quad (15)$$

The produced hydrogen is subsequently stored in specialized tanks for future utilization, while the oxygen is released into the atmosphere. In this research, excess generated energy will be utilized from the proposed system to supply the electrolyzer the required electrical power to operate. The rate of mass flow of the produced hydrogen can be determined using equation(16) (Baghaee et al., 2016):

$$\dot{m}H_2 = \frac{\eta_{Ez} P_{EZ}}{HHV_{H_2}} \quad (16)$$

Where η_{Ez} represents electrolyzer efficiency, HHV_{H_2} is hydrogen's higher heating hydrogen value, P_{EZ} is the electrical power input utilized by the electrolyzer.

According to (Falama et al., 2023) the power consumed by the electrolyzer P_{EZ} is given by equation (17):

$$P_{EZ}(t) = \frac{P_{excess}(t)}{\eta_{inv}} \quad (17)$$

The electrolyzer nominal power is given by equation (18) (Falama et al., 2023):

$$P_{EZ,n} = \frac{max\{P_{excess}(t)\}}{\eta_{inv}} \quad (18)$$

With $P_{excess}(t) = P_{PV}(t) + P_{WT}(t) - P_L(t)$ representing proposed system's produced excess energy, η_{inv} is the inverter efficiency.

2.4.6 Hydrogen tank modeling

With the proposed system, when the produced power from RES is higher than the required load, the load is fulfilled by the combined output of PV and wind, and any excess electricity is directed towards charging the battery. Otherwise, the excess electricity is utilized to generate hydrogen for the purpose of storage in the hydrogen storage tank (HT). The hydrogen tank capacity is given by the equation (19) (Mehrjerdi, 2019):

$$C_{HT}(t) = C_{HT}(t-1) + \dot{m}H_2(t) - \dot{L}H_2(t) \quad (19)$$

Where $\dot{L}H_2(t)$ hydrogen's load. The hydrogen tanks, when in operation, are subject to the following constraints, equation (20) (Mehrjerdi, 2019):

$$C_{HT\_min} \leq C_{HT}(t) \leq C_{HT\_max} \quad (20)$$

Where C_{HT_min} is the minimum capacity of the hydrogen tank and C_{HT_max} is the maximum allowable limit.

The hydrogen tank's state of charge (SOC_{H_2}) at any time t is determined by the equation (21) (Falama et al., 2023):

$$SOC_{H_2}(t) = SOC_{H_2}(t)(t-1) + \frac{P_{EZ}(t) \cdot \Delta t \cdot \eta_{EZ}}{C_{H_{2,n}}} + \frac{P_{FC}(t) \cdot \Delta t}{\eta_{EZ} \cdot C_{H_{2,n}}} \quad (21)$$

According to (Amara et al., 2021; H2data, n.d.), 1 kilogram of hydrogen is equivalent to 33.33 kilowatt-hours (kWh), the hydrogen tank nominal capacity in kWh is given by the equation (22):

$$C_{H_{2,n}} = Coef_{H_{2\_tank}} \times C_{H_{2\_unit}} \times 33.33 \quad (22)$$

$C_{H_{2\_unit}}$ represents HT unit capacity, equal to 1 kg and $Coef_{H_{2\_tank}}$ is the HT multiplication factor.

2.4.8 Fuel Cell modeling

With the proposed in case of the combined energy output from PV, wind, and the battery energy storage (BES) cannot fulfill the required load demand i.e. ($P_{PV}(t) + P_{WT}(t) + P_{BES}(t) < P_{load}(t)$), the fuel cell (FC) produces the additional power necessary to fulfill the energy requirement, i.e., ($P_{FC}(t) = P_{load}(t) - P_{PV}(t) - P_{WT}(t) - P_{BES}(t)$).

According to (Falama *et al.*, 2023) the fuel cell's instantaneous power output is determined by the equation (23):

$$P_{FC}(t) = \frac{P_{deficit}(t)}{\eta_{FC} \cdot \eta_{inv}} \quad (23)$$

And the nominal power of the FC is given by the equation (24):

$$P_{FC,n} = \frac{max\{P_{deficit}(t)\}}{\eta_{FC} \cdot \eta_{inv}} \quad (24)$$

Where ($P_{deficit}(t) = P_{load}(t) - P_{PV}(t) - P_{WT}(t) - P_{BES}(t)$)is the power produced by the FC when the RES, and BES production cannot supply the required load demand, η_{FC} is the FC efficiency.

2.4.6 Diesel Generator modeling

In this proposed model, when the out power from RES, BES, and FC unable to supply the load requirement, i.e., ($P_{PV}(t) + P_{WT}(t) + P_{FC}(t) + P_{BES}(t) < P_{load}(t)$), the missing load will be satisfied by the Diesel Generator (DG). When designing the proposed PV/Wind/FC/BES/DG system, the fuel consumption per hour and efficiency of the DG should be considered (Mouachi et al., 2020). The expression of the DG fuel usage at a specific time (t) is computed using equation (25) (Wankouo Ngouleu *et al.*, 2023b; Ouedraogo *et al.*, 2015):

$$F_G(t) = A_G \times P_{G\_out}(t) + B_G \times P_{G\_rated} \quad (25)$$

Where $F_G(t)$ is the consumed fuel by the DG at the time t (L/h), P_{G_rated} represents DG nominal power (Kw), $P_{G\_out}(t)$ the DG's output power at time t (Kw), while A_G and B_G denote the user-defined coefficients for the curve representing fuel consumption (Liter/kWh). In this study we considered AG=0.246L/kwh and BG =0.0845L/kwh (Hamanah *et al.*, 2020), and the efficiency of the DG is calculated utilizing equation (26) (Mouachi *et al.*, 2020; Azoumah *et al.*, 2011):

$$\eta_{overall} = \eta_{Brakethermal} \times \eta_{Generator} \quad (26)$$

Here $\eta_{overall}$: represents the overall efficiency and $\eta_{Brakethermal}$: signifies the brake thermal efficiency of the DG.

Equation (27) gives the yearly fuel cost (Wankouo Ngouleu et al., 2023b):

$$Fuel_{Cost} = Fuel_{Price} \times \sum_{t=1}^{8760} F_G(t) \quad (27)$$

The use of DG in HRES produced several greenhouse gas emissions (GHG) such as carbon dioxide (CO_2), Nitrogen oxides (NOX), carbon monoxide (CO), and Sulphur dioxide (SO_2) (Jamshidi et al., 2021).

In this study, we calculated the yearly avoided CO_2 by the proposed system instead GHG emissions given that CO_2 makes up the largest share of GHG emissions originating from the electricity sector and diesel uses (Cardenas *et al.*, 2022). To find the yearly avoided CO_2 by the proposed system, we deducted the total CO_2 emission of DG. The annual total emission of CO_2 by the DG is evaluate using equation (28) (Wankouo Ngouleu *et al.,* 2023b):

$$Total_{DGCO_{2emission}} = \varepsilon_{CO_2} \times \sum_{t=1}^{8760} F_G(t) \quad (Kg/year) \quad (28)$$

Where ε_{CO_2} (assumed to 2.7 kg/L) is the CO_2 emission rate measured in kg/L (Jamshidi et al., 2021).

2.5 Annualized cost analysis

The annual cost of a component can be computed using the Capital Recovery Factor (CRF). The CRF is employed to assess the current value, enhancing the economic precision calculations. The CRF is given by the equation (29) (Baghaee *et al.*, 2016; Wankouo Ngouleu *et al.*, 2023a):

$$CRF = \frac{i_r \cdot (1+i_r)^N}{(1+i_r)^N - 1} \quad (29)$$

Where i_r is represents the interest rate (we consider 10% in this study), N represents the lifespan of the systems component.

The annualized cost of the key components of the proposed system is by the equations (37) – (37) (Gangopadhyay *et al.*, 2024; Yimen et al., 2020; Yimen et al., 2020):

$$PV_{Cost} = N_{PV} \cdot [(C_{PV} \cdot CRF) + PV_{OM}] \quad (30)$$

$$WT_{Cost} = N_{WT} \cdot [(C_{WT} \cdot CRF) + WT_{OM}] \quad (31)$$

$$Inv_{Cost} = Inv_{size} \cdot [(C_{Inv} \cdot CRF) + Inv_{OM}] \quad (32)$$

$$Bat_{Cost} = N_{Bat} \cdot [(C_{Bat} + Rep_{cost}) \cdot CRF + Bat_{OM}] \quad (33)$$

$$EZ_{Cost} = N_{EZ} \cdot [(C_{EZ} + Rep_{cost}) \cdot CRF + EZ_{OM}] \quad (34)$$

$$HT_{Cost} = N_{HT} \cdot [(C_{HT} \cdot CRF) + HT_{OM}] \quad (35)$$

$$FC_{Cost} = N_{FC} \cdot [(C_{FC} + Rep_{cost}) \cdot CRF + FC_{OM}] \quad (36)$$

Table 2
Input parameters values utilized in optimization processes

Components	Rate capacity	Efficiency	Initial cost	Maintenance cost	Life time
PV	0.330 KW	17.01%	270 $	20$/year	20 years
Wind turbine	0.5 kW	96%	2000 $	60$/year	20 years
Battery	1.35 kWh	85%	130 $	10$/year	10 years
Electrolyzer	3 kW	74%	20000 $	1400$/kW	5 years
Fuel cell	3 kW	50%	20000 $	1400$/kW	5 years
H2 tank	1 kWh	95%	2000 $	0	20 years
Inverter	3 kW	95%	1500 $	0	10 years
Diesel Generator	3 kW	80%	500 $	0.10 $/hour	43800 h
Fuel	-	-	1$/L	-	-
Inflation rate	10%				
Project	-	-	-	-	20 years

Sources : (Wankouo Ngouleu *et al.*, 2023a; Baruah *et al.,* 2021; Ramesh & Saini, 2020; Alonso *et al.,* 2023; Wankouo Ngouleu *et al.,* 2023b)

$$DG_{Cost} = [(DG_{size} \cdot CRF) + DG_{OM} + Fuel_{cost}] \quad (37)$$

Where C_{PV} is the capital cost of solar modules, PV_{OM} is the solar modules' operation and maintenance, N_{PV} represents the solar modules' number, C_{WT} is the wind turbines' capital cost, WT_{OM} represents the wind turbines' maintenance and operation cost, N_{WT} is the wind turbines number, C_{Inv} is the inverter capital cost, Inv_{OM} represents the inverter's operation and maintenance cost, Inv_{size} is the rated inverter power, C_{Bat} is the battery capital cost, Bat_{OM} is the battery unit cost of operation and maintenance, N_{Bat} is the number of the battery units, C_{FC} is the fuel cell capital cost, FC_{OM} represents the fuel cell cost of maintenance and operation, N_{FC} is the fuel cell's number, C_{EZ} is the electrolyzer's capital cost , EZ_{OM} is represents electrolyser's maintenance and operation cost, N_{EZ} is the electrolyzer number, C_{HT} is the HT's capital cost, HT_{OM} represents HT's operation and maintenance cost, N_{HT} is the hydrogen storage tank number, DG_{cost} is the DG capital cost per KW, $DG_{OM_{cost}}$is the DG's operation and maintenance cost, and DG_{size} represents the DG's rated capacity.

The equation (38) provides the total yearly cost of the proposed system :

$$Total_{an_{cost}} = PV_{cost} + WT_{cost} + Inv_{cost} + Bat_{cost} + EZ_{cost} + HT_{cost} + FC_{cost} + DG_{cost} \quad (38)$$

Table 2 presents a summary of the input parameters utilized in this study throughout the optimization rocedure.

2.6 Evaluation of the criteria considered by the study

2.6.1 Criteria of evaluation

In this study, we consider four (4) main criteria (technical, economic, environmental, and social) and fourteen (14) sub-criteria (Figure 5) to optimally size the proposed system that maximizes the utilization of (PV/Wind/Fuel cell/battery) power output while minimizes the cost, and minimize as much as possible the use of DG. For the technical criteria, five (5) sub-criteria have been considered: The System Self-Consumption Index (SSCI), the System Self-Sufficiency Index (SSSI), the Loss of Load Probability (LOLP), the unmet load, and the energy excess. For the economic criteria, we considered the Net Present cost (NPC), the Levelized Cost of Energy (LCOE), the Levelized Cost of Hydrogen (LCOH), and the fuel cost.

The environmental criteria evaluate the avoided carbon dioxide (CO_2) and the renewable energy fraction. The new job creation opportunity, the Human Development Index (HDI) improvement, and the social acceptance have been considered as social criteria. The details of all the sub-criteria mentioned above and their mathematical models are presented in the following sections.

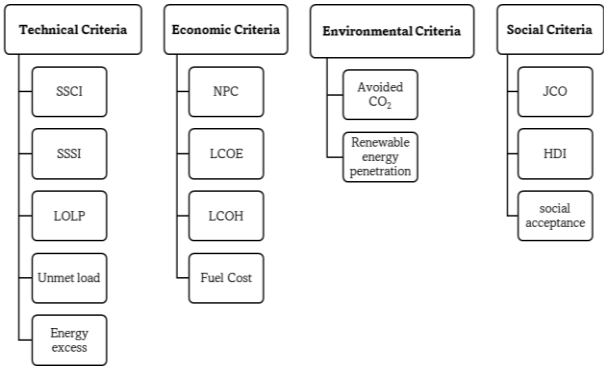

Fig. 5 Criteria considered for the evaluation of the proposed system

2.6.2 Technical criteria

2.6.2.1 System Self-Consumption Index (SSCI)

The SSCI measures how much energy generated by RES is consumed directly by the load demand rather than exported to the grid (Ciocia et al., 2021). A higher SSCI indicates more self-consumption and less grid dependence. The SSCI calculates the proportion between the instantaneous load demand that directly matches with the produced power by RES and the total generated energy by RES at interval T (Lombardi et al., 2018; Sokolnikova et al., 2020) equation (39):

$$SSCI = \frac{\int_0^T min\{P_{load}(t), P_T(t)\}dt}{\int_0^T P_T(t)dt} \quad (39)$$

2.6.2.2 System Self-Sufficiency Index (SSSI)

The SSSI measures how much of a system's energy demand is met by its own generation rather than imported from the grid or other sources. A higher SSSI means higher system self-sufficiency and lower dependence on external energy sources (Dufo-López *et al.*, 2016). The SSSI calculates the proportion between the amount of load requirement which directly corresponds to the power produced by RES, and covers the total load demand over the period T (Lombardi *et al.*, 2018; Sokolnikova *et al.*, 2020) equation (40). SSSI can be employed to assess the performance and benefits of net-zero energy systems or multi-energy systems, which generate electricity entirely from RES and convert it into alternative energy forms to meet multi-energy load (Dufo-López *et al.*, 2016; Lombardi *et al.,*

2018). SSSI can also forecast energy security and greenhouse gas emission reductions (Lombardi *et al.*, 2018).

$$SSSI = \frac{\int_0^T min\{P_{load}(t), P_T(t)\}dt}{\int_0^T P_{load}(t)dt} \quad (40)$$

2.6.2.3 Loss of Load Probability (LOLP)

The LOLP calculates the duration during which RES fail to fulfill the load requirement at the targeted reliability level (Lombardi *et al.*, 2018; Sokolnikova *et al.*, 2020) equation (41). LOLP is one of the generation system reliability indices that can be utilised to evaluate the economic and ecological advantages of RES, energy storage system (ESS), and grid export or import (Ascend Analytics, n.d.).

$$LOLP = \frac{\sum_1^t P_{deficit}(t)}{8760} \cdot 100\% \quad (41)$$

2.6.2.4 Unmet load (UL)

The UL is defined as the ratio of the annual non-serviced load to the total annual load, as indicated in the equation (42) (Mandal *et al.*, 2018; Khan *et al.*, 2021):

$$Unmet\ load = \frac{Annual\ Non\ served\ Load}{Annual\ Entire\ \ Load} \quad (42)$$

2.6.3 Economic criteria

2.6.3.1 Net Present cost (NPC)

The NPC represents the initial Total Annualized Cost (TAC) ratio by the Total CRF at the project's onset (Uwineza *et al.,* 2022; Masrur *et al.*, 2020) equation (43):

$$NPC = \frac{Total_{ancost}}{CRF(i_r, N)} \quad (43)$$

Where i_r is the yearly real rate of interest in percentage (%), and N is the project lifespan.CRF is expressed in equation (29) (Ghenai & Bettayeb, 2019; Uwineza *et al.*, 2022).

2.6.3.2 Levelized Cost of Energy (LCOE)

The LCOE ($/kWh) is calculated by dividing the TAC by the total annual electrical load served (Uwineza *et al.*, 2022; Mandal *et al.*, 2018; Ajlan *et al.*, 2017) equation (44):

$$LCOE = \frac{Total_{ancost}}{\sum_{t=1}^{8760} P_{load}(t)} \quad (44)$$

2.6.3.3 Levelized Cost of Hydrogen (LCOH)

The LCOH ($/kWh) is calculated by dividing the TAC sum by the total yearly hydrogen load provided (Bhandari & Shah, 2021; Nasser *et al.*, 2022) equation (45):

Table 3
Factor for emissions of greenhouse gases

Greenhouse Gas	Emission factor value	Unit
SO_X	0.5	gSOx/ kWh
NO_X	0.22	gNOx/ kWh
CO_2	690	gCO_2/ kWh

Sources: (Peng *et al.*, 2013; Ackermann *et al.*, 2001)

Table 4
Job creation factor of the various components

Components	Job Creation Factor
Battery	0.01 job/MWh
Electrolyzer/Hydrogen tank/Fuel cell	0.5 job/MWe
PV generator	2.70 jobs/MW
Wind	1.10 jobs/MW

Sources: (BHAGWAT & OLCZAK, 2020; Hassan *et al.*, 2022; Ram *et al.*, 2020; Hondo & Moriizumi, 2017)

$$LCOH = \frac{Total_{ancost}}{\sum_{t=1}^{8760} H_{load}(t)} \quad (45)$$

2.6.4 Environmental criteria

2.6.4.1 Avoided carbon dioxide (CO_2)

Avoided CO_2 refers to the quantity of CO_2 emissions prevented from accessing the atmosphere due to using renewable energy sources rather than fossil fuels (Alshammari & Asumadu, 2020; EIA, n.d. ; Kabeyi & Olanrewaju, 2022), the yearly avoided CO_2 is expressed by the equation (46):

$$Avoided_{CO_2} = (SO_X + NO_X + CO_2) \cdot (0.001) \cdot \sum_{t=1}^{8760} P_{load}(t)\, dt \quad (46)$$

Total yearly avoided CO_2 in Kg (0.001 factor to convert g to Kg) Where SOx, NOX, and CO_2 are emission factor for the greenhouse gas respectively sulfur oxides, nitrogen oxides, and carbon dioxide.
Table 3 gives the different values of the emission factor of greenhouse gas.

2.6.4.2 Renewable energy penetration (REP)

REP measures the percentage of RES in the total energy supply of the system as presented in equation (47). A higher REP means a higher share of RES and a lower dependence on fossil fuels (Ramli *et al.*, 2018; Khan *et al.*, 2021; Bukar *et al.*, 2019). Thus, an REP value close to 100% is more desirable.

$$REP = 100 \cdot \left[1 - \left(\frac{\sum_{t=1}^{8760} P_{deficit}(t)}{\sum_{t=1}^{8760} P_{load}(t)}\right)\right] \quad (47)$$

2.6.5 Social criteria

2.6.5.1 Job creation opportunity (JCO)

The proposed system's job creation opportunity is calculated considering the job creation of each component of the technology that constitutes the proposed system. It is expressed by the equation (48) (Dufo-López *et al.*, 2016; Cameron & Van Der Zwaan, 2015; Sawle *et al.*, 2018):

$$JCO = JC_{PV} \cdot P_{PV} + JC_{WT} \cdot P_{WT} + JC_{Bat} \cdot E_{Bat} + (N_{FC} + N_{EZ} + HT_{PC} + N_{H_2}) \cdot JC_{EZH_2FC} \quad (48)$$

Where JC_{PV}, JC_{WT}, JC_{Bat}, and JC_{EZH2FC} are respectively the job creation factors of PV, Wind, Battery and electrolyzer/ hydrogen/fuel cell. P_{PV} is the maximum power of the PV, P_{WT} is the maximum power of wind turbine, E_{Bat} is the nominal capacity of the battery, N_{FC} is the fuel cell number, N_{EZ} is the

electrolyzer number, HT_{PC} is the hydrogen tank power capacity, and the N_{H2} is the hydrogen tank number.
Table 4 shows the job creation factor of the various proposed system's components.

2.6.5.2 Human Development Index (HDI)

A mentioned in the section 2.1 CHAD is one of the countries that has an HDI that is too low (0.398), ranking it 187th out of 189 in the world. In this study the developed model considers the HDI.

We consider that the annual energy excess from RES (Table 5), which was not taken into account when defining the load and that cannot be stored in the battery or utilized to produce hydrogen, can be utilized to launch new services, businesses or small workshops that can enhance the quality of life therefore the HDI. The HDI can be formulated as follows (Sawle *et al.*, 2018; Dufo-López *et al.*, 2016) equation (49).

$$HDI = 0.0978ln\left[\sum_{t=1}^{8760} P_{load}(t) + min\left(F_{maxSE} \cdot \sum_{t=1}^{8760} E_{dump,F_{maxload}} \cdot \sum_{t=1}^{8760} P_{load}(t)\right) / \eta_{per}\right] - 0.0319F_{maxSE} \quad (49)$$

Where Edump is the annual energy excess transferred to the grid, *Fmax*SE is a factor utilized to calculate the maximum Edump that could be utilized by additional unexpected AC load demand, F*max*load presents the factor multiplied by the yearly AC load demand to ensure that the surplus energy consumed by unexpected AC does not exceed the required load, η_{per} is number of persons residing is studied location. In this study we consider that all energy excess will be transferred to the grid for loads *Fmax*SE = 100% that do not exceed 75% of current load demand, F*max*load = 0.75.

2.7 Formulation of the optimization problem

2.7.1 Optimization method

We used the MATLAB R2023b environment to implement a MOPSO algorithm to design the proposed system. Originally, Kenedy and Eberhart developed the PSO algorithm, which was utilized to solve multi-objective and non-linear complex problems (Alshammari & Asumadu, 2020). The PSO algorithm is a powerful optimization technique modeled on social behaviors observed in animals, like the flocking of birds and schooling of fish, and operates on a population-based approach (Ma & Yuan, 2023). PSO is a popular optimization method due to its simple concept and ability to find quickly an optimal solution. It is commonly utilized in hybrid renewable energy system sizing (El Boujdaini *et al.*, 2022). Figure 6 represents he pseudo-code of the PSO (Ma & Yuan, 2023) and Figure 7 shows the optimal sizing of the proposed system utilizing the PSO algorithm.

2.7.2 Objective functions and constraints

To evaluate the economic viability, the higher self-sufficiency and the lower dependence on external energy sources of the proposed system, the ASC and the SSSI, respectively, were chosen as objective functions (OF).

Step 1. Initialization

for each particle:

initialize position and velocity randomly

calculate fitness function

initialize p_{best} to its initial position

initialize g_{best} to the minimal value of the swarm

Step 2. Repeat until a stopping criterion is satisfied:

for each particle:

update position and velocity matrices

evaluate the fitness function

while (i < maximum iterations)

Step 3. post process the result

Fig. 6 Pseudo-code for PSO

The OF and the constraints of the variables under consideration in this study are respectively expressed in equations (50) and (52) (Uwineza *et al.*, 2022; Rosenstiel *et al.*, 2021; Ming *et al.*, 2017):

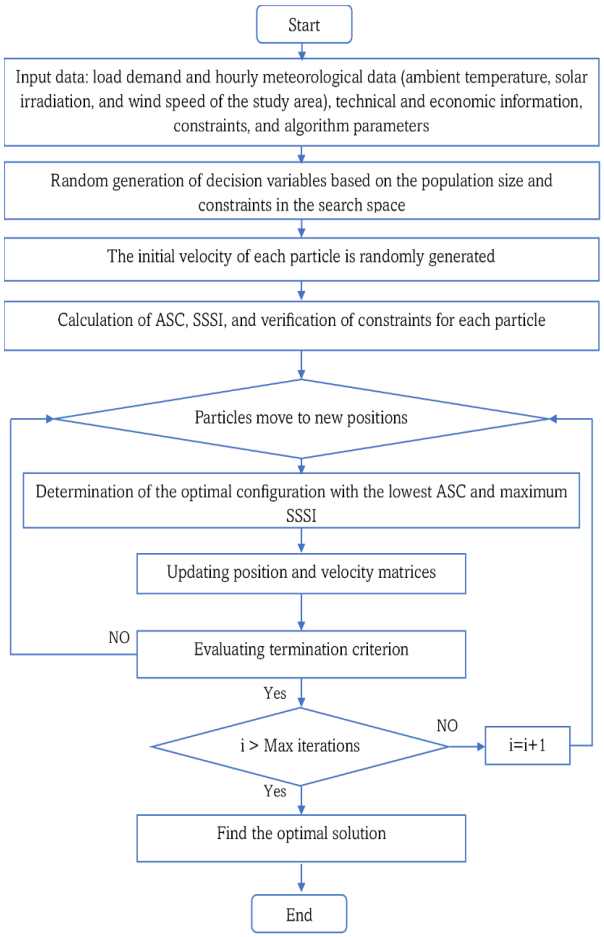

Fig. 7 Application of the PSO in the proposed system's optimal design

$$OF = \begin{cases} Min(ASC) = f(PV, WT, Bat, EZ, HT, FC, DG) \\ Max(SSSI) = f(PV, WT, Bat, EZ, HT, FC, DG) \end{cases} \quad (50)$$

Subject to:

$$\begin{cases} 20\% \leq SOC_{Bat} \leq 100\% \\ 5\% \leq SOC_{HT} \leq 100\% \\ N_x^{min} \leq N_x \leq N_x^{max} = \{PV, WT, Bat, EZ, HT, FC, DG\} \end{cases} \quad (51)$$

Where SOC_{HT}, SOC_{Bat}, N_x^{min}, N_x, N_x^{max} are respectively hydrogen tank and battery's state of charge, and Nx represent proposed system's number of components.

3. Results and discussion

This present section discusses the results of the proposed system's optimal sizing (PV/Wind/Battery/FuelCell/DG) considering technical, economic, environmental, and social criteria.

3.1 Optimal sizing results and energy management analysis

Energy management describes the control strategy developed in 2.3.2 and the optimized system's energy and power flows. This subsection presents and analyzes the results of the optimal sizing and energy management of the proposed system (PV/Wind/BES/FC/DG).

Figure 8 below shows the pareto front optimal solutions for the variation of system self-sufficiency Index (SSSI) against annualized cost of the system (ACS). SSSI is a measure of system reliability while ACS is an economic assessment index of the system. As outlined in the methodology details in Figures 6 and 7 above, when the reproduction is done for maximum iterations and the fitness solution does not improve further, the MOPSO generates the optimal pareto front solutions for the proposed sizing technique as shown in Figure 8. The trend is attributed to the tricky balance between the system reliability (SSSI) and the system economics (ACS). Our study established the best system reliability (SSSI) of about 56.87 % (~57%) with a system economic value of (ACS) of 153891$ while the best system economic value 158177$ at a system reliability of 45.41% (~45%). Thus, the proposed system should have a reliability of 51.14 % (average of the best system reliability and reliability at the best system economic value) and an economic value of 156034$ (average of the best economic value and the economic value at the best system reliability).

Table 5
Optimal sizing of the proposed system

Optimal solutions	
Wind Turbine (KW)	166
Total Wind Energy (kWh)	166340
Solar Power (KW)	493
Total Solar Energy (kWh)	820020
Battery Energy Charge (KWh)	229180
Battery Energy Discharge (KWh)	221300
Electrolyzer size (KW)	202
Number of Hydrogen Tanks	997
Hydrogen Energy (KWh)	83874
Fuel Cell size (KW)	144
Fuel Cell output Energy (kWh)	41937
Total DG Energy (kWh)	0
DG size	0
DG emissions (Kg)	0
Total Load demand (kWh)	542390

Table 5 shows the proposed system's optimal regarding each component's power and energy and the total load demand. From Table 5, to meet the total load demand of 542,390 KWh, we note that in terms of energy source, the load is primarily satisfied by solar with a power of 493 KW, followed by the wind turbine with a power of 166 KW. Regarding the contribution of storage to meeting load demand, the battery is at the head with an energy supply of 221,300 KWh, followed by hydrogen with a contribution of 83,874 kWh. As stated in point 2.3.1, one of the objectives of this research is to maximize the use of solar, wind, battery, and hydrogen, respectively, and minimize the use of diesel generators (DG) as much as possible. Thus, Table 5 clearly shows that the contribution of DG is zero with zero CO_2 emissions.

Figure 9 (a) and (b) represents the daily production of the solar and wind turbines, with a maximum output of 323 KW at noon for the PV and a maximum production of 104 KW for the wind turbine at 10 am. The minimum output is 32 KW at 7 am for the wind turbine and zero between 1-6 am, 6 pm, and midnight for the PV.

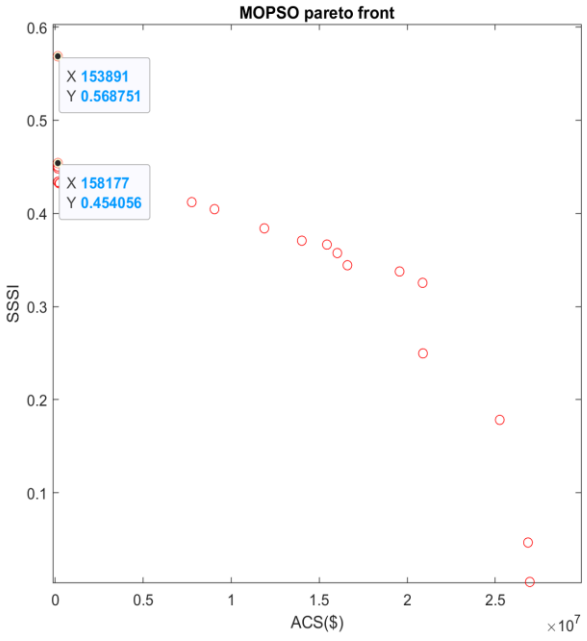

Fig. 8 Plot of SSSI against ASC showing the pareto front solution

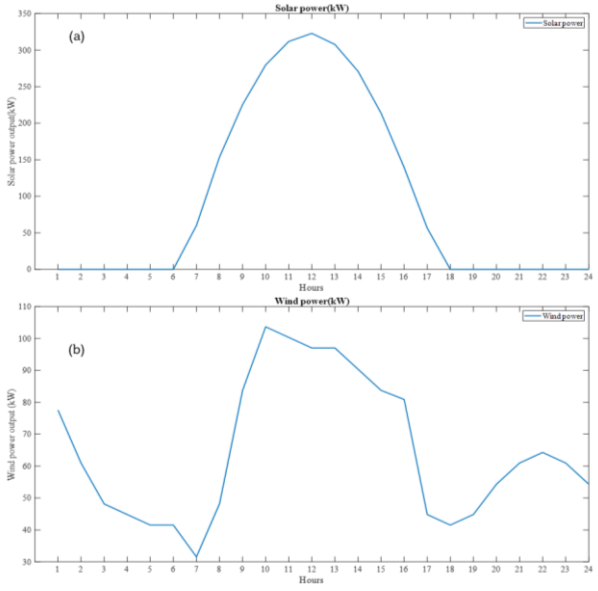

Fig. 9 Plot of daily solar power output (a) and wind power output (b) versus hours for the study area

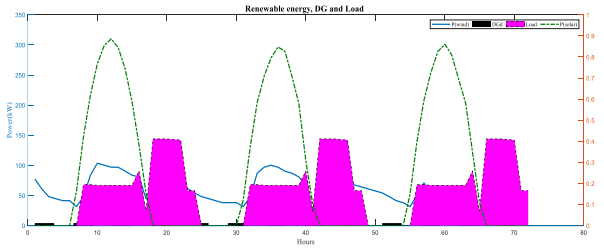

Fig. 10 Difference between the total renewable energy generated power, DG and the load

The effect of solar irradiation and wind speed variations can explain the maximum and minimum outputs of solar and wind turbines. As shown in Figure 2, the maximum solar irradiance is 1017 W/m^2 at noon, corresponding to the maximum output of PV (323 KW) in Figure 9. In the same way, the maximum wind speed of 4.14 m/s observed at 10 a.m. in Figure 2 corresponds to the maximum output of a wind turbine (104 KW) in Figure 9. We can also explain the minimum production of the solar and wind turbines in the same way: the minimum solar irradiance of 0 (between 1-6 a.m., 6 p.m., and midnight) and wind speed (2.62 m/s at 7 a.m.) observed in Figure 2 correspond to the minimum of solar PV and wind turbines, respectively in Figure 9.

Figure 10 illustrates the disparity between the total output of PV, wind, and DG and the considered load requirement for three (3) consecutive days. From Figure 10, we notice that during the three (3) days, the production of PV and wind is significantly higher than the load demand between 6 a.m. and 6 p.m. At the same time, the load demand is greater than the PV and wind generation every day between 6 p.m. and 10 p.m., corresponding to the peak of the load demand. We also note that the production of the wind turbine is greater than the load demand during day 1 (between 11 p.m. and 6 a.m.) and day 2 (between 11 p.m. and 7 a.m.). and on day 3, the PV production alone is higher than the load demand between 6 a.m. and 6 p.m. DG production is zero during the three (3) days.

Both the photovoltaic solar production (which is only available during the day) and the wind power production are irregular and do not always correspond to the peak load demand, as observed in Figure 10. Thus, both lead to a mismatch between production and load demand. Therefore, energy storage devices are essential to supply electricity to the village at any time, whether annually or daily, for more reliable energy availability. At a given time, t, of the day, the difference between the total power generated from renewable energy sources and the load demand is derived from $\Delta P(t) = \left(P_{PV}(t) + P_{WT}(t)\right) - P_{load}(t)$ and the storage must fulfill this difference. In this study, we used batteries and hydrogen as storage options. Figures 11-13 show the annual battery charge /discharge, hydrogen tank energy status, and the annual produced hydrogen and converted into electricity. These

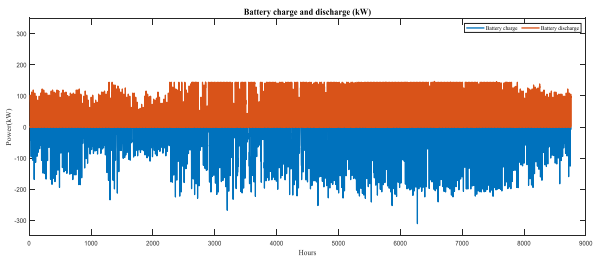

Fig. 11 Annual battery input and output

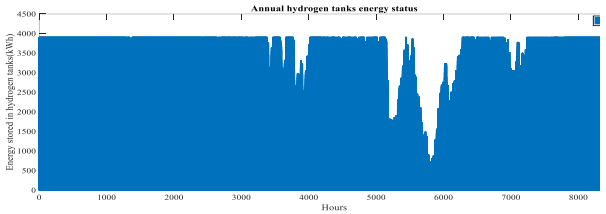

Fig. 12 Annual hydrogen tank energy status

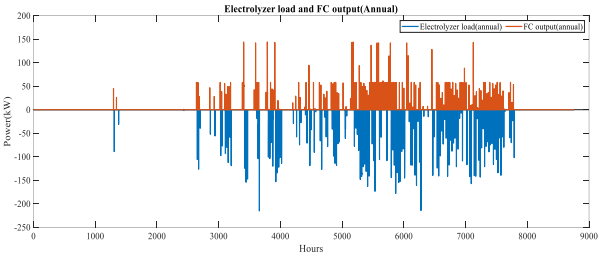

Fig. 13 Annual electrolyzer load and Fuel cell output

figures show the annual contribution of each storage option to the satisfaction of load demand.

The energy excess from renewable energy sources (solar and wind) observed in Figure 10 (between 6 a.m. and 6 p.m. for solar) and (between 11 p.m. and 6 a.m. for wind) will be stored in the storage devices (as shown in Figures 11 and 12). As per our control strategy described in 2.3.2, Case 1, this energy excess was used to charge the battery (Figure 11); otherwise, the excess will be utilized for hydrogen production to store in the hydrogen tank (Figure 12). In Case 2, if the battery is fully charged, the hydrogen tank is also filled, and the output of renewable energy sources fulfills the load demand, then surplus energy is dumped. This excess energy can be used for other businesses and applications such as heating, cooling, and ventilation. In this study, the algorithm will use the amount of dumped energy to calculate the Human Development Index using equation 49 (as described in 2.6.5.2).

The complementarity of resources of the proposed system (PV/Wind/battery/FC) makes the system more reliable for energy availability on an annual or daily scale, eco-friendly, and environmentally efficient. Figures 14 and 15 illustrate the comparison over three (3) days of different combinations of sources. Figures 14 and 15 show that no solar power is produced (between 1-6 a.m., 6 p.m., and midnight) due to the unavailability of solar irradiance, as explained in Figures 9 (a) and 2. At this moment, the wind turbine is the only renewable energy source working to meet the load demand. When the wind turbine's power output is insufficient, as observed in Figures 14 during the peak demand hours (between 6 p.m. and 10 p.m.), the energy previously stored in the battery (Figure 11) and hydrogen tank (Figure 12) will be used to meet the deficit between renewable power sources and the load demand. As per the developed control strategy (2.3.2), the battery is discharged (Figure 11) to fulfill the load demand. At this moment, the algorithm prioritizes the wind and the battery to satisfy the energy demand (Figure 14). In the case of the wind, the battery cannot fulfill the load demand, so the fuel cell uses the stored hydrogen from hydrogen tanks to fill the gap between the load and the produced power (Figure 13). If the power from solar, wind, fuel cells, and batteries cannot match the energy demand, the diesel generator is purchased to provide the missing load demand. Due to the high fuel cost and environmental impact of using a diesel generator (DG), in this study, we minimize the use of DG (DG = 0) throughout the year. According to Figures 14–

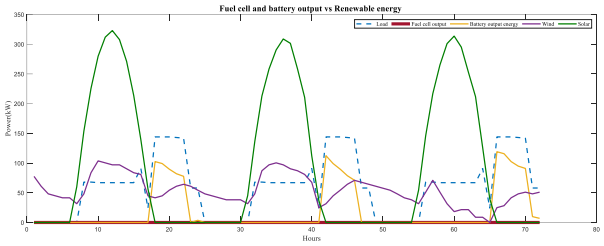

Fig. 14 Renewable Energy Vs Fuel cell and battery output

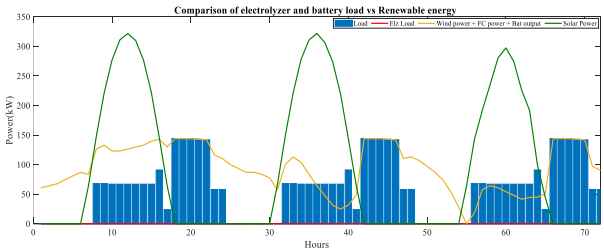

Fig. 15 Comparison of electrolyzer and battery load Vs Renewable Energy

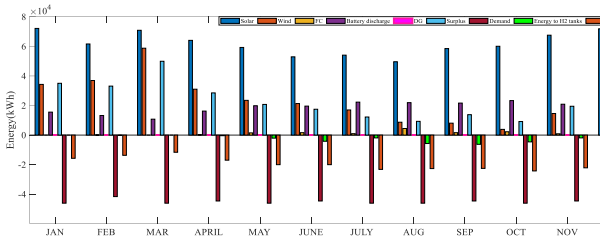

Fig. 16 Proposed system's yearly energy status

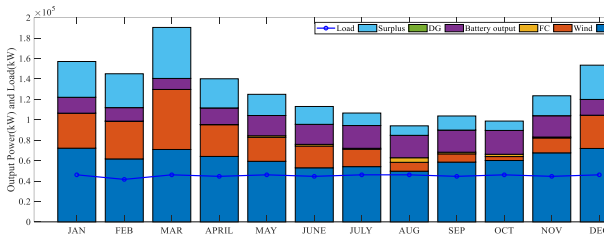

Fig. 17 Annual power status of the proposed system

17 and the results of Table 5, the output power of DG is zero, with zero CO_2 emissions. Figure 15 shows clearly that the load requirement is fulfilled at any time by the complementarity and combination of battery output, fuel cell output, solar, and wind.

Additionally, Figures 14 and 15 show that when solar irradiation is available between 6 a.m. and 6 p.m., the combined power from solar and wind turbines far exceeds the load demand. The excess energy is used to charge the battery (Figure 11); otherwise, it goes through the electrolyzer to produce hydrogen (Figure 13), which is stored in hydrogen tanks until it reaches full charge (Figure 11). When the battery is fully charged, the hydrogen tanks are full, and the load demand is satisfied, the excess from renewable energy is dumped and recorded as "excess energy." The algorithm will consider this dumped energy in this study in the calculation of the Human Development Index.

The proposed system's annual energy and power output status for each system element and their contribution to fulfilling the load demand by month, the surplus energy, and DG are shown in Figures 16 (energy vs months) and 17 (power vs months). Figures 16 and 17 show that solar production is dominant throughout the year due to the high solar irradiation, as seen in Figure 2. Wind production is low between July and November due to the low wind speed in the study area during this interval (rainy season). We also note the contribution of the battery throughout the year, while the contribution of hydrogen is only noted between May and November. This phenomenon is explained by the management strategy that we implemented. The algorithm first prioritizes solar and wind to satisfy the load demand. Then, if solar and wind production cannot meet the load demand, the algorithm prioritizes the battery to fill the gap. Finally, if solar, wind, and battery output power cannot meet the load demand, the algorithm calls on hydrogen to satisfy the demand. Figures 16 and 17 also show the contribution of diesel generation is zero throughout the year for the same reasons explained previously.

In practice, 1.3% of Chad's rural population with access to electricity uses diesel generators (DG) to meet their electricity demand. These DG are often inefficient and challenging to maintain, leading to regular power outages in rural areas. Furthermore, there is a need to transport fuel to these locations. Together, these problems contribute to an expensive electricity production system. Consequently, taking into account the difficulties encountered by the 1.3% of the rural population of Chad who already have access to electricity and to provide access to electricity to the 98.7% of the rural population who have not yet access to electricity using hybrid renewable energy sources can be a hopeful alternative. Thus, the government, private institutions, and stakeholders can use this study as a decision tool.

3.2 Technical criteria results analysis

We will analyze and evaluate the technical criteria results considered during the optimal modelling of the proposed system in this subsection. The developed strategy impacts the technical criteria because one objective function is maximizing the System Self-Sufficiency Index (SSSI). Table 6 displays the optimal results of the technical criteria. There is no load loss, as mentioned in the operational strategy, which is implemented to ensure that the load will always be supplied (LOLP = 0 and Unmet load = 0). By using the proposed operational strategy 28.39% of the produced electricity by RES can be directly integrated to supply the load requirement (SSCI = 28.39%) and 51.63% of the power produced by RES is utilized to charge the battery and produce green hydrogen then to convert it into electricity to satisfy the load requirement when the RE cannot meet it (SSSI = 51.63%). As mentioned in section 2.6.2.2 a higher SSSI means higher proposed system self-sufficiency and lower dependence on external energy sources.

Table 6
Optimal results of the technical criteria

Technical results	
SSCI (%)	28.39
SSSI (%)	51.14
LOLP (%)	0
Unmet load	0
Excess Energy (kWh)	290090

Table 7
Optimal results of the economic criteria

Economic results	
NPC ($)	2298500
LCOE ($/kWh)	0.2982
LCOH ($/kg)	3.8563
Fuel cost ($/L)	0

3.3 Economic criteria results analysis

Table 7 shows the optimal findings of the proposed system's economic criteria for the considered load demand. The proposed system's NPC is 2298500$, the results reveal that the optimal sizing gives the lowest LCOE (0.2982$/kWh) compared to the previous works done in Chad by HOMER Pro (0.30 €/kWh=0.32$/kWh) (Hassane, Didane et al., 2022), and (0.507 $/kWh) (Jahangiri *et al.*, 2019) with different systems configurations. The found LCOE is 51.12% lower than the national unit production costs of the electricity in rural areas of CHAD, which is 0.61 $/kWh (Abdelhamid, 2023). These optimal results give also low LCOH (3.8563 $/kg) compared to (Jahangiri *et al.*, 2019).

3.4 Environmental criteria results analysis

Table 8 shows the environmental criteria results, which are the avoided CO_2 (Kg) and the renewable energy fraction (%). The annual CO_2 avoided by the proposed system is 374640kg (374. 640 tonnes), which will help Chad meet its commitments made during the 2015 Paris Agreement, which included an overall mitigation target of 19.3% compared to the reference scenario, i.e., 16,372 kt CO_2 eq to be avoided by 2030. The energy sector is the most targeted by less polluting actions in producing and consuming electrical energy based on renewable energies, natural gas, and energy efficiency (Abdelhamid, 2023). Currently, the national energy consumption is dominated by 96.5% by the consumption of wood fuels (wood and charcoal), with disastrous consequences for the forest cover and the environment. The RES fraction in the proposed system is 100%, with 17% Wind turbine fraction and 83% Solar fraction. Therefore, with this high percentage in RE, the proposed system provides and improve access to cost-effective, reliable, and sustainable energy to the rural areas of Chad and also a solution to the consequences of climate change to which Chad is exposed.

3.5 Social criteria results analysis

The social criteria obtained values while optimizing the proposed system by the implemented PSO algorithm are displayed in Table 9. This study considered three social criteria: the job creation opportunity (JCO), the HDI, and social acceptance. This study is one of the fist studies evaluating these social criteria in the Chadian context. According to the results of the social criteria obtained from the simulation, the proposed system will create five (5) direct jobs and improve the HDI by 17.66% (Table 9). The obtained HDI is 0.4683, and the Chad HDI is 0.398 (PNUD, 2020). Concerning the 3rd evaluation criterion, which is the social acceptance, we referred to the field survey carried out by (Hassane, Didane *et al.*, 2022) on accessibility to renewable energies in Chad; 95% of the surveyed individuals expressed a positive inclination towards adopting or transitioning to renewable energy systems.

Table 8
Optimal results of the environmental criteria

Environmental results	
Avoided CO_2 (Kg)	374640
Renewable Energy fraction (%)	100
Solar PV fraction (%)	17
Wind turbine fraction (%)	83

Table 9
Optimal results of the social criteria

Social results	
Job Creation Opportunity (JCO)	5
Human Development Index (HDI)	0.4683 (CHAD HDI =0.398)

4. Conclusions

In this study, we performed a techno-economic, environmental, and social multi-criteria hybrid system based on optimal sizing of solar photovoltaics, wind turbines, batteries, fuel cells, and diesel generators for rural electrification in Chad. To fulfill this purpose, we used three types of load profiles that can be identified as a typical example of a non-electrified rural area of Chad, choosing the village of KOUNDOUL (11° 58′ 35″ North, 15° 09′ 00″ East) as a case study. Hourly meteorological data (ambient temperature, solar irradiation, and wind speed) of the study area collected from the Photovoltaic Geographical Information System (PVGIS) website, as well as the techno-economic characteristics of components of the proposed system, have been used for this purpose.

The MATLAB R2023b environment has been used to implement and run a multi-objective Particle Swarm Optimization (MOPSO) algorithm to solve the main optimization problem of the proposed system. The objective is to find the optimal sizing of the proposed system by defining the installed capacities of the PV, Wind, Battery, electrolyzer, hydrogen tank, and fuel cell while minimizing the Annualized System Cost (ASC) and maximizing the system self-sufficiency index (SSSI), and obtaining the values of the other sub-criteria representing the technical, economic, environmental, and social criteria, which are decision variables for this feasibility study.

The simulation results demonstrate that the optimal sizing of the proposed fulfills the load demand at annual and daily scales by complementarity and combination of the different resources. In this study, we also analyzed the simulation results of the technical, economic, environmental, and social criteria, respectively, and the results showed significant improvement in social, environmental, economic, and system reliability. This study could help designers, companies, investors, policymakers, and the government of Chad in making decisions when implementing such a system in particular rural areas. It could also provide a better practical energy design tool.

Acknowledgments

The authors acknowledge the Regional Scholarship for Innovation Fund (RSIF) - Partnership for Skills in Applied Sciences, Engineering, and Technology (PASET) for the financial support.

Author Contributions: Mahamat Adoum Abdoulaye: Conceptualization, Methodology, Software, Validation, Formal analysis, Investigation, Resources, Writing – original draft, Writing – review & editing, Visualization. Sebastian Waita: Conceptualization, Methodology, Writing - review, Supervision. Cyrus Wekesa Wabuge: Conceptualization, Methodology, Writing - review, Supervision. Julius Mwakondo Mwabora: Conceptualization, Methodology, Writing - review, Supervision.

Funding: Funding for this research was provided by RSIF – PASET

Conflicts of Interest: The authors declare that they have no known conflict of interest interests or personal relationships that could have appeared to influence the work reported in this paper.

References

Abdelhamid, I. H. (2023). These de doctorat/Ph.D, Promotion des énergies renouvelables pour réduire l'impact environnemental du Tchad à travers sa balance énergétique : cas du solaire et de l'éolien. *UNIVERSITE DE DOUALA (Laboratory of Energy,*

Materials, Modeling and Methods).

Ajlan, A., Tan, C. W., & Abdilahi, A. M. (2017). Assessment of environmental and economic perspectives for renewable-based hybrid power system in Yemen. *Renewable and Sustainable Energy Reviews*, *75*(November 2016), 559–570. https://doi.org/10.1016/j.rser.2016.11.024

Al-Buraiki, A. S., & Al-Sharafi, A. (2022). Hydrogen production via using excess electric energy of an off-grid hybrid solar/wind system based on a novel performance indicator. *Energy Conversion and Management*, *254*(January), 115270. https://doi.org/10.1016/j.enconman.2022.115270

Albertus, P., Manser, J. S., & Litzelman, S. (2020). Long-Duration Electricity Storage Applications, Economics, and Technologies. *Joule*, *4*(1), 21–32. https://doi.org/10.1016/j.joule.2019.11.009

Alshammari, N., & Asumadu, J. (2020). Optimum unit sizing of hybrid renewable energy system utilizing harmony search, Jaya and particle swarm optimization algorithms. *Sustainable Cities and Society*, *60*(March), 102255. https://doi.org/10.1016/j.scs.2020.102255

Amara, S., Toumi, S., Salah, C. Ben, & Saidi, A. S. (2021). Improvement of techno-economic optimal sizing of a hybrid off-grid micro-grid system. *Energy*, *233*, 121166. https://doi.org/10.1016/j.energy.2021.121166

Anoune, K., Bouya, M., Astito, A., & Abdellah, A. Ben. (2018). Sizing methods and optimization techniques for PV-wind based hybrid renewable energy system: A review. *Renewable and Sustainable Energy Reviews*, *93*(April), 652–673. https://doi.org/10.1016/j.rser.2018.05.032

Ascend Analytics. (n.d.). *Loss of Load Probability: Application to Montana*. 1–7.

Ayop, R., & Tan, C. W. (2017). A comprehensive review on photovoltaic emulator. *Renewable and Sustainable Energy Reviews*, *80*(January), 430–452. https://doi.org/10.1016/j.rser.2017.05.217

Aziz, A. S., Tajuddin, M. F. N., Adzman, M. R., Azmi, A., & Ramli, M. A. M. (2019). Optimization and sensitivity analysis of standalone hybrid energy systems for rural electrification: A case study of Iraq. *Renewable Energy*, *138*, 775–792. https://doi.org/10.1016/j.renene.2019.02.004

Azoumah, Y., Yamegueu, D., Ginies, P., Coulibaly, Y., & Girard, P. (2011). Sustainable electricity generation for rural and peri-urban populations of sub-Saharan Africa: The "flexy-energy" concept. *Energy Policy*, *39*(1), 131–141. https://doi.org/10.1016/j.enpol.2010.09.021

Baghaee, H. R., Mirsalim, M., Gharehpetian, G. B., & Talebi, H. A. (2016). Reliability/cost-based multi-objective Pareto optimal design of stand-alone wind/PV/FC generation microgrid system. *Energy*, *115*, 1022–1041. https://doi.org/10.1016/j.energy.2016.09.007

Bahramara, S., Moghaddam, M. P., & Haghifam, M. R. (2016). Optimal planning of hybrid renewable energy systems using HOMER: A review. *Renewable and Sustainable Energy Reviews*, *62*, 609–620. https://doi.org/10.1016/j.rser.2016.05.039

BHAGWAT, S., & OLCZAK, M. (2020). Green hydrogen : bridging the energy transition in Africa and Europe. In *FSR Global* (Issue October). https://cadmus.eui.eu/handle/1814/68677

Bhandari, R., & Shah, R. R. (2021). Hydrogen as energy carrier: Techno-economic assessment of decentralized hydrogen production in Germany. *Renewable Energy*, *177*, 915–931. https://doi.org/10.1016/j.renene.2021.05.149

Bocklisch, T. (2015). Hybrid energy storage systems for renewable energy applications. *Energy Procedia*, *73*, 103–111. https://doi.org/10.1016/j.egypro.2015.07.582

Bukar, A. L., Tan, C. W., & Lau, K. Y. (2019). Optimal sizing of an autonomous photovoltaic/wind/battery/diesel generator microgrid using grasshopper optimization algorithm. *Solar Energy*, *188*(June), 685–696. https://doi.org/10.1016/j.solener.2019.06.050

Cameron, L., & Van Der Zwaan, B. (2015). Employment factors for wind and solar energy technologies: A literature review. *Renewable and Sustainable Energy Reviews*, *45*, 160–172. https://doi.org/10.1016/j.rser.2015.01.001

Cardenas, G. A. R., Khezri, R., Mahmoudi, A., & Kahourzadeh, S. (2022). Optimal Planning of Remote Microgrids with Multi-Size Split-Diesel Generators. *Sustainability (Switzerland)*, *14*(5). https://doi.org/10.3390/su14052892

Casati, P., Moner-Girona, M., Shehu, I. K., Szabó, S., & Nhamo, G. (2023). Datasets for a multidimensional analysis connecting clean energy access and social development in sub-Saharan Africa. *Data in Brief*, *47*, 108948. https://doi.org/10.1016/j.dib.2023.108948

Ciocia, A., Amato, A., Leo, P. Di, Fichera, S., Malgaroli, G., Spertino, F., & Tzanova, S. (2021). *Systems : Effect of Grid Limitation and Storage Installation*.

Delano, O., Odou, T., Bhandari, R., & Adamou, R. (2020). Hybrid off-grid renewable power system for sustainable rural electri fi cation in Benin. *Renewable Energy*, *145*, 1266–1279. https://doi.org/10.1016/j.renene.2019.06.032

Diaf, S., Diaf, D., Belhamel, M., Haddadi, M., & Louche, A. (2007). *A methodology for optimal sizing of autonomous hybrid PV / wind system*. *35*(11), 5708–5718. https://doi.org/10.1016/j.enpol.2007.06.020

Diop, M., Sow, S., Pabame, Z., Ndiaye, A., & Kébé, C. M. F. (2019). Technical, Economic and Environmental Analysis of Hybrid Energy Solutions for Rural Electrification in the Republic of Chad. *Lecture Notes of the Institute for Computer Sciences, Social-Informatics and Telecommunications Engineering, LNICST*, *296*, 26–37. https://doi.org/10.1007/978-3-030-34863-2_3

Djounga, B. A. (2023). *Planning and implementation of a sustainable, decentralized village electricity access program: Case study of Ourda Community – Chad*.

Dufo-López, R., Cristóbal-Monreal, I. R., & Yusta, J. M. (2016). Optimisation of PV-wind-diesel-battery stand-alone systems to minimise cost and maximise human development index and job creation. *Renewable Energy*, *94*, 280–293. https://doi.org/10.1016/j.renene.2016.03.065

EIA, U. S. E. I. A. (n.d.). *How much carbon dioxide is produced per kilowatthour of U.S. electricity generation?*

El Boujdaini, L., Mezrhab, A., Moussaoui, M. A., Jurado, F., & Vera, D. (2022). Sizing of a stand-alone PV–wind–battery–diesel hybrid energy system and optimal combination using a particle swarm optimization algorithm. *Electrical Engineering*, *104*(5), 3339–3359. https://doi.org/10.1007/s00202-022-01529-0

Emad, D., El-Hameed, M. A., & El-Fergany, A. A. (2021). Optimal techno-economic design of hybrid PV/wind system comprising battery energy storage: Case study for a remote area. *Energy Conversion and Management*, *249*, 114847. https://doi.org/10.1016/j.enconman.2021.114847

Falama, R. Z., Saidi, A. S., Souloukngа, M. H., & Salah, C. Ben. (2023). A techno-economic comparative study of renewable energy systems based different storage devices. *Energy*, *266*(June 2022), 126411. https://doi.org/10.1016/j.energy.2022.126411

Fu, X. (2022). Statistical machine learning model for capacitor planning considering uncertainties in photovoltaic power. *Protection and Control of Modern Power Systems*, *7*(1). https://doi.org/10.1186/s41601-022-00228-z

Gangopadhyay, A., Seshadri, A. K., & Patil, B. (2024). Wind-solar-storage trade-offs in a decarbonizing electricity system. *Applied Energy*, *353*(PA), 121994. https://doi.org/10.1016/j.apenergy.2023.121994

Ghenai, C., & Bettayeb, M. (2019). Modelling and performance analysis of a stand-alone hybrid solar PV/Fuel Cell/Diesel Generator power system for university building. *Energy*, *171*, 180–189. https://doi.org/10.1016/j.energy.2019.01.019

Guangqian, D., Bekhrad, K., Azarikhah, P., & Maleki, A. (2018). A hybrid algorithm based optimization on modeling of grid independent biodiesel-based hybrid solar/wind systems. *Renewable Energy*, *122*, 551–560. https://doi.org/10.1016/j.renene.2018.02.021

H2data. (n.d.). http://www.h2data.de/ [Accessed on October 19, 2023]

Hamanah, W. M., Abido, M. A., & Alhems, L. M. (2020). Optimum Sizing of Hybrid PV, Wind, Battery and Diesel System Using Lightning Search Algorithm. *Arabian Journal for Science and Engineering*, *45*(3), 1871–1883. https://doi.org/10.1007/s13369-019-04292-w

Hassan, R., Das, B. K., & Hasan, M. (2022). Integrated off-grid hybrid renewable energy system optimization based on economic, environmental, and social indicators for sustainable development. *Energy*, *250*, 123823. https://doi.org/10.1016/j.energy.2022.123823

Hassane, A. I., Ali, A. H. M., Tahir, A. M., & Hauglustaine, J. M. (2019). Simulation of a photovoltaic panels market for promoting solar energy in Chad. *International Journal of Renewable Energy Research*, *9*(3), 1472–1469. https://doi.org/10.20508/ijrer.v9i3.9377.g7741

Hassane, A. I., Didane, D. H., Tahir, A. M., & Hauglustaine, J. M. (2018). Wind and solar assessment in the Sahelian zone of Chad. *International Journal of Integrated Engineering*, *10*(8), 164–174. https://doi.org/10.30880/ijie.2018.10.08.026

Hassane, A. I., Didane, D. H., Tahir, A. M., Hauglustaine, J. M., Manshoor, B., Batcha, M. F. M., Tamba, J. G., & Mouangue, R. M. (2022). Techno-economic feasibility of a remote PV mini-grid electrification system for five localities in Chad. *International Journal of Sustainable Engineering*, *15*(1), 179–193. https://doi.org/10.1080/19397038.2022.2101707

Hassane, A. I., Didane, D. H., Tahir, A. M., Mouangue, R. M., Tamba, J. G., & Hauglustaine, J. M. (2022). Comparative analysis of hybrid renewable energy systems for off-grid applications in chad. *International Journal of Renewable Energy Development*, *11*(1), 49–62. https://doi.org/10.14710/ijred.2022.39012

Hondo, H., & Moriizumi, Y. (2017). Employment creation potential of renewable power generation technologies: A life cycle approach. *Renewable and Sustainable Energy Reviews*, *79*(August 2016), 128–136. https://doi.org/10.1016/j.rser.2017.05.039

Islam, M. R., Akter, H., Howlader, H. O. R., & Senjyu, T. (2022). Optimal Sizing and Techno-Economic Analysis of Grid-Independent Hybrid Energy System for Sustained Rural Electrification in Developing Countries: A Case Study in Bangladesh. *Energies*, *15*(17). https://doi.org/10.3390/en15176381

Jahangiri, M., Souloukngа, M. H., Bardei, F. K., Shamsabadi, A. A., Akinlabi, E. T., Sichilalu, S. M., & Mostafaeipour, A. (2019). Techno-econo-environmental optimal operation of grid-wind-solar electricity generation with hydrogen storage system for domestic scale, case study in Chad. *International Journal of Hydrogen Energy*, *44*(54), 28613–28628. https://doi.org/10.1016/j.ijhydene.2019.09.130

Jamshidi, S., Pourhossein, K., & Asadi, M. (2021). Size estimation of wind/solar hybrid renewable energy systems without detailed wind and irradiation data: A feasibility study. *Energy Conversion and Management*, *234*(January), 113905. https://doi.org/10.1016/j.enconman.2021.113905

Kaabeche, A., & Ibtiouen, R. (2014). Techno-economic optimization of hybrid photovoltaic/wind/diesel/battery generation in a stand-alone power system. *Solar Energy*, *103*, 171–182. https://doi.org/10.1016/j.solener.2014.02.017

Kabeyi, M. J. B., & Olanrewaju, O. A. (2022). Sustainable Energy Transition for Renewable and Low Carbon Grid Electricity Generation and Supply. In *Frontiers in Energy Research* (Vol. 9). Frontiers Media S.A. https://doi.org/10.3389/fenrg.2021.743114

Kelly, E., Medjo Nouadje, B. A., Tonsie Djiela, R. H., Kapen, P. T., Tchuen, G., & Tchinda, R. (2023). Off grid PV/Diesel/Wind/Batteries energy system options for the electrification of isolated regions of Chad. *Heliyon*, *9*(3). https://doi.org/10.1016/j.heliyon.2023.e13906

Khan, F. A., Pal, N., & Saeed, S. H. (2021). Optimization and sizing of SPV/Wind hybrid renewable energy system: A techno-economic and social perspective. *Energy*, *233*, 121114. https://doi.org/10.1016/j.energy.2021.121114

Kharrich, M., Mohammed, O. H., & Akherraz, M. (2019). Assessment of renewable energy sources in Morocco using economical feasibility technique. *International Journal of Renewable Energy Research*, *9*(4), 1856–1864. https://doi.org/10.20508/ijrer.v9i4.10181.g7791

Kharrich, M., Mohammed, O. H., Alshammari, N., & Akherraz, M. (2021). Multi-objective optimization and the effect of the economic factors on the design of the microgrid hybrid system. *Sustainable Cities and Society*, *65*(October 2020), 102646. https://doi.org/10.1016/j.scs.2020.102646

Koholé, Y. W., Djiela, R. H. T., Fohagui, F. C. V., & Ghislain, T. (2023). Comparative study of thirteen numerical methods for evaluating Weibull parameters for solar energy generation at ten selected locations in Cameroon. *Cleaner Energy Systems*, *4*(November 2022), 100047. https://doi.org/10.1016/j.cles.2022.100047

León Gómez, J. C., De León Aldaco, S. E., & Aguayo Alquicira, J. (2023). A Review of Hybrid Renewable Energy Systems: Architectures, Battery Systems, and Optimization Techniques. *Eng*, *4*(2), 1446–1467. https://doi.org/10.3390/eng4020084

Li, C. H., Zhu, X. J., Cao, G. Y., Sui, S., & Hu, M. R. (2009). Dynamic modeling and sizing optimization of stand-alone photovoltaic power systems using hybrid energy storage technology. *Renewable Energy*, *34*(3), 815–826. https://doi.org/10.1016/j.renene.2008.04.018

Li, J., Liu, P., & Li, Z. (2022). Optimal design and techno-economic analysis of a hybrid renewable energy system for off-grid power supply and hydrogen production: A case study of West China. *Chemical Engineering Research and Design*, *177*, 604–614. https://doi.org/10.1016/j.cherd.2021.11.014

Lombardi, P., Arendarski, B., Suslov, K., Shamarova, N., Sokolnikova, P., Pantaleo, A. M., & Komarnicki, P. (2018). A Net-Zero Energy System Solution for Russian Rural Communities. *E3S Web of Conferences*, *69*. https://doi.org/10.1051/e3sconf/20186901013

Ma, J., & Yuan, X. (2023). Techno-economic optimization of hybrid solar system with energy storage for increasing the energy independence in green buildings. *Journal of Energy Storage*, *61*(December 2022), 106642. https://doi.org/10.1016/j.est.2023.106642

Maklewa Agoundedemba. (2023). Energy Status in Africa: Challenges, Progress and Sustainable Pathways. *Energies,16, 7708*.

Mandal, S., Das, B. K., & Hoque, N. (2018). Optimum sizing of a stand-alone hybrid energy system for rural electrification in Bangladesh. *Journal of Cleaner Production*, *200*, 12–27. https://doi.org/10.1016/j.jclepro.2018.07.257

Masrur, H., Howlader, H. O. R., Lotfy, M. E., Khan, K. R., Guerrero, J. M., & Senjyu, T. (2020). Analysis of techno-economic-environmental suitability of an isolated microgrid system located in a remote island of Bangladesh. *Sustainability (Switzerland)*, *12*(7). https://doi.org/10.3390/su12072880

Mbainaissem Peurdoum Richard (Consultant National au PNUD, A. E. (2014). *Rapport national du tchad*.

Mehrjerdi, H. (2019). Off-grid solar powered charging station for electric and hydrogen vehicles including fuel cell and hydrogen storage. *International Journal of Hydrogen Energy*, *44*(23), 11574–11583. https://doi.org/10.1016/j.ijhydene.2019.03.158

Mouachi, R., Jallal, M. A., Gharnati, F., & Raoufi, M. (2020). *Multiobjective Sizing of an Autonomous Hybrid Microgrid Using a Multimodal Delayed PSO Algorithm : A Case Study of a Fishing Village. 2020*.

Mumtaz, F., Zaihar Yahaya, N., Tanzim Meraj, S., Singh, B., Kannan, R., & Ibrahim, O. (2021). Review on non-isolated DC-DC converters and their control techniques for renewable energy applications. *Ain Shams Engineering Journal*, *12*(4), 3747–3763. https://doi.org/10.1016/j.asej.2021.03.022

Nasser, M., Megahed, T. F., Ookawara, S., & Hassan, H. (2022). Techno-economic assessment of clean hydrogen production and storage using hybrid renewable energy system of PV/Wind under different climatic conditions. *Sustainable Energy Technologies and Assessments*, *52*(PB), 102195. https://doi.org/10.1016/j.seta.2022.102195

Olivetti, E. A., Ceder, G., Gaustad, G. G., & Fu, X. (2017). Lithium-Ion Battery Supply Chain Considerations: Analysis of Potential Bottlenecks in Critical Metals. *Joule*, *1*(2), 229–243. https://doi.org/10.1016/j.joule.2017.08.019

Ouedraogo, B. I., Kouame, S., Azoumah, Y., & Yamegueu, D. (2015). Incentives for rural off grid electrification in Burkina Faso using LCOE. *Renewable Energy*, *78*, 573–582. https://doi.org/10.1016/j.renene.2015.01.044

PNUD. (2020). *Élargir l'horizon des populations et de la planète : le développement humain et l'Anthropocène / Rapport sur le développement humain 2020*. http://hdr.undp.org/en/data.

Ram, M., Aghahosseini, A., & Breyer, C. (2020). Job creation during the global energy transition towards 100% renewable power system by 2050. *Technological Forecasting and Social Change*, *151*(September 2018), 119682. https://doi.org/10.1016/j.techfore.2019.06.008

Ramli, M. A. M., Bouchekara, H. R. E. H., & Alghamdi, A. S. (2018). Optimal sizing of PV/wind/diesel hybrid microgrid system using multi-objective self-adaptive differential evolution algorithm. *Renewable Energy*, *121*, 400–411. https://doi.org/10.1016/j.renene.2018.01.058

Sawle, Y., Gupta, S. C., & Bohre, A. K. (2018). Socio-techno-economic design of hybrid renewable energy system using optimization techniques. *Renewable Energy*, *119*, 459–472. https://doi.org/10.1016/j.renene.2017.11.058

Shafiullah, G. M., Masola, T., Samu, R., Elavarasan, R. M., Begum, S., Subramaniam, U., Romlie, M. F., Chowdhury, M., & Arif, M. T. (2021). Prospects of Hybrid Renewable Energy-Based Power System: A Case Study, Post Analysis of Chipendeke Micro-

Hydro, Zimbabwe. *IEEE Access*, *9*, 73433–73452. https://doi.org/10.1109/ACCESS.2021.3078713

Singh, S., Chauhan, P., Aftab, M. A., Ali, I., Suhail Hussain, S. M., & Ustun, T. S. (2020). Cost Optimization of a Stand-Alone Hybrid Energy System with Fuel Cell and PV. *Energies 2020, Vol. 13, Page 1295*, *13*(5), 1295. https://doi.org/10.3390/EN13051295

Sokolnikova, P., Lombardi, P., Arendarski, B., Suslov, K., Pantaleo, A. M., Kranhold, M., & Komarnicki, P. (2020). Net-zero multi-energy systems for Siberian rural communities: A methodology to size thermal and electric storage units. *Renewable Energy*, *155*, 979–989. https://doi.org/10.1016/j.renene.2020.03.011

Talla Konchou, F. A., Djeudjo Temene, H., Tchinda, R., & Njomo, D. (2021). Techno-economic and environmental design of an optimal hybrid energy system for a community multimedia centre in Cameroon. *SN Applied Sciences*, *3*(1), 1–12. https://doi.org/10.1007/s42452-021-04151-0

The World Bank Group. (2021). World Development Indicators | DataBank. In *DataBank - World Development Indicators*. https://databank.worldbank.org/indicator/NY.GDP.MKTP.KD.ZG/1ff4a498/Popular-Indicators%0Ahttp://databank.worldbank.org/data/reports.aspx?source=world-development-indicators

Uwineza, L., Kim, H. G., Kleissl, J., & Kim, C. K. (2022). Technical Control and Optimal Dispatch Strategy for a Hybrid Energy System. *Energies*, *15*(8), 1–19. https://doi.org/10.3390/en15082744

Wang, Z., Wang, Q., Zhang, Z., & Razmjooy, N. (2021). A new configuration of autonomous CHP system based on improved version of marine predators algorithm: A case study. *International Transactions on Electrical Energy Systems*, *31*(4), 1–22. https://doi.org/10.1002/2050-7038.12806

Wankouo Ngouleu, C. A., Koholé, Y. W., Fohagui, F. C. V., & Tchuen, G. (2023a). Optimal sizing and techno-enviro-economic evaluation of a hybrid photovoltaic/wind/diesel system with battery and fuel cell storage devices under different climatic conditions in Cameroon. *Journal of Cleaner Production*, *423*(September). https://doi.org/10.1016/j.jclepro.2023.138753

Wankouo Ngouleu, C. A., Koholé, Y. W., Fohagui, F. C. V., & Tchuen, G. (2023b). Optimal sizing and techno-enviro-economic evaluation of a hybrid photovoltaic/wind/diesel system with battery and fuel cell storage devices under different climatic conditions in Cameroon. *Journal of Cleaner Production*, *423*(May). https://doi.org/10.1016/j.jclepro.2023.138753

Wu, Q., Fan, Z., Zhang, J., Sun, Q., & Yang, J. (2019). Optimization Design and Simulation of Microgrid in Amdjarass Town, Chad. *E3S Web of Conferences*, *118*. https://doi.org/10.1051/e3sconf/201911802015

Xu, Y., Pei, J., Cui, L., Liu, P., & Ma, T. (2022). The Levelized Cost of Storage of Electrochemical Energy Storage Technologies in China. *Frontiers in Energy Research*, *10*(June), 1–16. https://doi.org/10.3389/fenrg.2022.873800

Yimen, N., Tchotang, T., Kanmogne, A., Idriss, I. A., Musa, B., Aliyu, A., Okonkwo, E. C., Abba, S. I., Tata, D., Meva'a, L., Hamandjoda, O., & Dagbasi, M. (2020). Optimal sizing and techno-economic analysis of hybrid renewable energy systems—a case study of a photovoltaic/wind/battery/diesel system in Fanisau, Northern Nigeria. *Processes*, *8*(11), 1–25. https://doi.org/10.3390/pr8111381

Zhang, G., Shi, Y., Maleki, A., & A. Rosen, M. (2020). Optimal location and size of a grid-independent solar/hydrogen system for rural areas using an efficient heuristic approach. *Renewable Energy*, *156*, 1203–1214. https://doi.org/10.1016/j.renene.2020.04.010

Zhang, Y., & Yu, Y. (2022). Carbon Value Assessment of Hydrogen Energy Connected to the Power Grid. *IEEE Transactions on Industry Applications*, *58*(2), 2803–2811. https://doi.org/10.1109/TIA.2021.3126691

https://doi.org/10.61435/ijred.2024.60169
ISSN: 2252-4940/© 2024.The Author(s). Published by CBIORE